

# **NUMERICAL ANALYSIS OF FREEZE-THAW PROCESSES OVER SEASONAL FROZEN GROUNDS: A CASE STUDY OVER MAQU, TIBETAN PLATEAU**

HONGYI CHEN

Feb, 2016

SUPERVISORS:

Dr. Yijian Zeng

Dr.Donghai Zheng

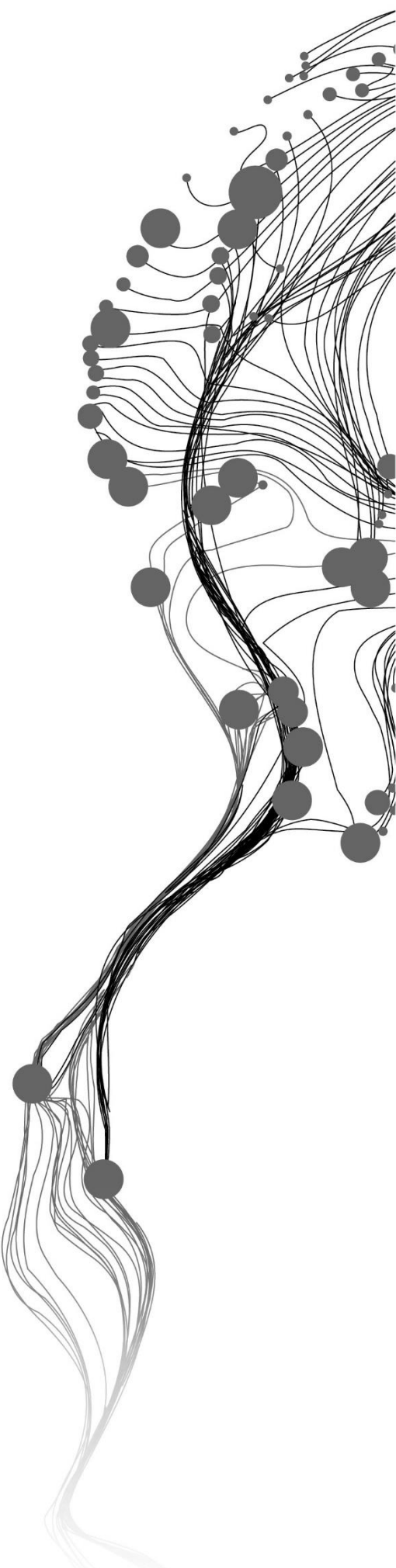
ADVISOR:

Dr.Rogier van der Velde

THESIS ASSESSMENT BOARD:

[Prof.Dr. Z. Su (Chair)]

[Dr. V. (Viktor) Bense (External Examiner, Wageningen  
University)]



# **NUMERICAL ANALYSIS OF FREEZE-THAW PROCESSES OVER SEASONAL FROZEN GROUNDS: A CASE STUDY OVER MAQU, TIBETAN PLATEAU**

HONGYI CHEN

Enschede, Netherlands, Feb, 2016

Thesis submitted to the Faculty of Geo-Information Science and Earth Observation of the University of Twente in partial fulfilment of the requirements for the degree of Master of Science in Geo-information Science and Earth Observation.

Specialization: [Water Resources and Environment Management]

**SUPERVISORS:**

Dr. Yijian Zeng

Dr. Donghai Zheng

**ADVISOR:**

Dr. Rogier van der Velde

**THESIS ASSESSMENT BOARD:**

[Prof. Dr. Z. Su (Chair)]

[Dr. V. (Viktor) Bense (External Examiner, Wageningen University)]

#### DISCLAIMER

This document describes work undertaken as part of a programme of study at the Faculty of Geo-Information Science and Earth Observation of the University of Twente. All views and opinions expressed therein remain the sole responsibility of the author, and do not necessarily represent those of the Faculty.

## ABSTRACT

The topic studied in this paper is to investigate the freeze-thaw processes in seasonal frozen grounds, with the simulation results generated from Noah Land Surface Model. The major issue, for this study, is to detect the amount of water at different phases (e.g. TSWC-total soil water content, LSWC-liquid soil water content& SIC-soil ice content), and to investigate the processes of freezing-thawing transitions in frozen soil at different depth of soil.

The approaches adopted to solve the problem are three steps. First of all, it is required to retrieve a long term observation data on soil moisture (SM) and soil temperature (ST), from the study area, Maqu, the eastern part of the source region of yellow river (SRYR). Then a pixel-wise validation is operated by using those observation data. After the validation, it was found the Noah LSM can represent the hydrothermal dynamics over the Maqu reasonably to a certain extent and can be used for further analysis. This study focuses on the evaluation of the performance of Noah LSM in calculating SIC, in order to understand the freeze-thaw transitions over the Maqu area.

The results obtained in this study, based on two sets of data, observed and simulated, includes Maqu Network in situ data of 20 station, and Noah LSM simulation results (between 2002 and 2011). Validation data consists of two sets, for one is the pixel-wise simulated data, 30 minutes interval, at 4 different depths (5 cm, 25 cm, 70 cm, and 160 cm). And the other is observation data organized at 10-min interval or 15 minutes intervals, varies at 5 different depths at 5 cm, 10 cm, 20 cm, 40 cm, and 80 cm.

It is illustrated from obtained results that LSM model is reliable at Maqu. The correlation coefficient between the simulation results and observations of SM and ST can reach over 0.8 for each validated pixel. Then the pixel-wise simulation results were assembled or averaged into one, to study the four variables, and especially the SIC, about their long term variation, lag time between different layers and Active Layer Thickness.

## ACKNOWLEDGEMENTS

All the gratefully thank you to my supervisors, Mr. YijianZeng and Mr. Donghai Zheng. You are my guild lights and turn me out of the trouble all the time.

All the gratefully thank you to my advisors, Dr.Rogier van der Velde.

All the gratefully thank you to thesis assessment board, Prof.Dr. Z. Su and Dr. V. (Viktor) Bense.

Thanks you to my parents and family, for your unconditional love all the time.

Thank you to my friends for accompanying me all the way.

Thank you to ITC for providing me a warmest help for the study at more than 14 months.

# TABLE OF CONTENTS

---

1.	Background.....	7
1.1.	Introduction .....	7
1.2.	Measurement.....	8
2.	Research problem.....	9
2.1.	Major interests .....	9
3.	Objectives and questions.....	10
3.1.	Objectives .....	10
3.2.	Sub-objectives .....	10
3.3.	Research Questions.....	10
4.	Study area .....	11
4.1.	Maqu observation station.....	11
4.2.	In-situ Datasets .....	12
5.	Methodology.....	13
5.1.	Noah Land Surface Model.....	13
5.2.	Noah LSM: Freeze-thaw process .....	14
5.3.	ECH <sub>2</sub> O probe .....	15
5.4.	Flowchart .....	15
6.	Validation Results and analysis.....	17
6.1.	Validation results .....	17
6.2.	Statistic results.....	18
6.3.	Validation results analysis .....	20
6.4.	Conclusion of validation .....	21
7.	Simulation results and analysis .....	23
7.1.	Soil moisture and soil temperature.....	23
7.2.	Liquid Water Content.....	26
7.3.	Soil ice content.....	27
7.4.	Active Layer Thickness .....	34
8.	Conclusion .....	37
8.1.	Review on the thesis .....	37
8.2.	Conclusions and subsequial work .....	37

# LIST OF FIGURES

---

FIGURE 1.1 VALIDATION RESULTS ON STATION CST05 (ROW 1 COLUMN 2) .....	41
FIGURE 1.2 VALIDATION RESULTS ON STATION NST04-NST05 (ROW 1 COLUMN 4) .....	42
FIGURE 1.3 VALIDATION RESULTS ON STATION CST02 (ROW 1 COLUMN 5) .....	42
FIGURE 1.4 VALIDATION RESULTS ON STATION NST11-NST12 (ROW 1 COLUMN 8) .....	43
FIGURE 1.5 VALIDATION RESULTS ON STATION NST03 (ROW 2 COLUMN 5).....	43
FIGURE 1.6 VALIDATION RESULTS ON STATION NST15 (ROW 3 COLUMN 2).....	43
FIGURE 1.7 VALIDATION RESULTS ON STATIONCST03 (ROW 3 COLUMN 3).....	44
FIGURE 1.8 VALIDATION RESULTS ON STATION NST14 (ROW 3 COLUMN 4).....	44
FIGURE 1.9 VALIDATION RESULTS ON STATION CST01 (ROW 3 COLUMN 5) .....	45
FIGURE 1.10 VALIDATION RESULTS ON STATION NST09- NST 10 (ROW 3 COLUMN 9) .....	45
FIGURE 1.11 VALIDATION RESULTS ON STATION NST13 (ROW 4 COLUMN 3).....	46
FIGURE 1.12 VALIDATION RESULTS ON STATION NST06 (ROW 4 COLUMN 6).....	46
FIGURE 1.13 VALIDATION RESULTS ON STATION NST07 (ROW 4 COLUMN 7).....	46
FIGURE 1.14 VALIDATION RESULTS ON STATION NST08 (ROW 4 COLUMN 9).....	47
FIGURE 2.1 SIMULATION RESULTS-LSWC .....	47
FIGURE 2.2 SIMULATION RESULTS-TSWC.....	47
FIGURE 2.3 SIMULATION RESULTS-SIC .....	47
FIGURE 2.4 SIMULATION RESULTS-ST .....	48
FIGURE 2.5 SIMULATION RESULTS AT DAILY AVERAGE-LSWC .....	48
FIGURE 2.6 SIMULATION RESULTS AT DAILY AVERAGE-TSWC .....	48
FIGURE 2.7 SIMULATION RESULTS AT DAILY AVERAGE-SIC.....	48
FIGURE 2.8 SIMULATION RESULTS AT DAILY AVERAGE-ST .....	49
FIGURE 2.9 3-DAY AVERAGE-LSWC.....	49
FIGURE 2.10 3-DAY AVERAGE-TSWC .....	49
FIGURE 2.11 3-DAY AVERAGE-SIC.....	49
FIGURE 2.12 3-DAY AVERAGE-ST .....	50
FIGURE 2.13 WEEKLY AVERAGE-LSWC .....	50
FIGURE 2.14 WEEKLY AVERAGE-TSWC .....	50
FIGURE 2.15 WEEKLY AVERAGE-SIC.....	50
FIGURE 2.16 WEEKLY AVERAGE-ST.....	51
FIGURE 2.17 MONTHLY AVERAGE-LSWC.....	51
FIGURE 2.18 MONTHLY AVERAGE-TSWC.....	51
FIGURE 2.19 MONTHLY AVERAGE-SIC .....	51
FIGURE 2.20 MONTHLY AVERAGE-ST .....	52
FIGURE 3.1 FLOWCHART .....	<b>ERROR! BOOKMARK NOT DEFINED.</b>
FIGURE 3.2 ACTIVE LAYER THICKNESS AT LONG TERM VARIATION .....	53

## LIST OF TABLES

---

TABLE 1.1 MONITORING STATIONS AND ITS LOCATING PIXELS.....	55
TABLE 2 .1 VALID SIC DATES OF THE SIMULATION RESULT .....	55
TABLE 2 .2 VALID SIC PERCENTAGE OF THE SIMULATION RESULT .....	55
TABLE 2.3 BOTTOM ST DATES OF THE SIMULATION RESULT .....	56
TABLE 2.4 BOTTOM ST AND LAG TIME OF THE SIMULATION RESULT ( DAYS ) .....	56
TABLE 2.5 SIC LAG TIME BETWEEN DIFFERENT LAYERS .....	56
TABLE 2.6 CONTINUOUS DURATION OF SIC OF DIFFERENT LAYERS (SOURCE DATA, WITH CONSTRAINT) .....	57
TABLE 2.7 CONTINUOUS DURATION OF SIC OF DIFFERENT LAYERS (DAILY AVERAGE, WITHOUT CONSTRAINT) .....	57
TABLE 2.8 CONTINUOUS DURATION OF SIC OF DIFFERENT LAYERS (SOURCE DATA, WITH CONSTRAINT) .....	58
TABLE 2.9 CONTINUOUS DURATION OF SIC OF DIFFERENT LAYERS (DAILY AVERAGE, WITH CONSTRAINT).....	58



# 1. BACKGROUND

## 1.1. Introduction

It is a common sense that pure water freezes at 0°C at atmospheric pressure. However, it is until recent decades that scientists start to recognize water is not completely condensed into ice in soil as soon as the so temperature falls below zero degree Celsius, but extends over a range along with the decreasing lines of temperature (Zreda, Desilets, Ferré, & Scott, 2008). In other words, liquid water and ice coexist at a certain range of sub-zero temperature in frozen soil (Baker & Lawson, 2006). When soil temperature gradually drops below the freezing point, a portion of water in the soil, mostly those in the large pores turn into ice. The remainder which in small capillaries exists as adsorbed films around soil particles, in pores with sufficiently small diameters and in crevices between soil particles. As the temperature continues to fall, more water becomes frozen, leaving residual liquid water in progressively thinner adsorbed films, smaller pores and crevices. Consequently, a small amount of soil water may remain in a liquid state at temperatures well below the freezing point of water (Spaans & Baker, 1995). The exact temperature when transition finished is not constant for the reason that the transition is strongly influenced by soil particles which is identified as soil texture, soil properties, for instance, bulk density of soil, and some other factors remain undiscovered.

The finer-grained and smaller-pored frozen soils generally have larger unfrozen water contents compared to coarser-grained and larger-pored frozen soils at the same negative temperature. For example, in fine-grained soil such as clay, a significant amount of water remains unfrozen even at a temperature of -22°C, while in coarse-grained soil, such as sand, water almost completely freezes at a temperature slightly below 0°C. The coexistence of water and ice in frozen soils affects hydraulic, thermal, and mechanical properties of frozen soils and thus has a significant influence on environmental processes. Due to the large amount of latent heat associated with the phase change, the freezing of water in the soil delays the winter cooling of the land surface, while thawing of ice in the frozen soil delays the summer warming of the land surface (Poutou, et al., 2004). The frozen soil affects soil hydrology by reducing the soil's hydraulic conductivity (Iwata et al., 2010), which in turn increases surface runoff relative to the unfrozen soil. The amount of ice content in frozen soil has a complicated influence on shear strength of frozen soil (Arenson, Johansen, & Springman, 2004) and thus stability of frozen steep slopes. Even very small changes in the amount of unfrozen water in frozen soil can dramatically alter the rheological properties (Arenson, Springman, & Segó, 2007).

The freeze–thaw process is a complicated in phase transition which refers to water and ice, the physical movement at vertical and horizontal direction, and mutual reaction with heat exchange and other factors act on surface.

Besides, it is widely accepted that the transport of water in partially frozen soils is governed by the same processes as that in unsaturated unfrozen soils (Harlan, 1973; Jame & Norum, 1980; Jame & Norum, 1980; Lundin, 1990) However, there has been opposite discussion on this topic. A disagreement about the effect of ice on hydraulic conductivity of frozen soil is announced by Kurylyk and Watanabe (2013), who believes an arbitrary fitting factor (impedance factor) is often employed to reduce hydraulic conductivity due to formation of ice. To date, there is no generally-accepted theory for simulating freezing and thawing processes in unsaturated soils.

Understanding the water exchange and energy cycling in a soil freezing–thawing process, it is of importance to account for the mechanism of water movement in frozen soil, the fluctuation of weather system recorded by ice and therefore, the feedbacks on the climate system in frigid environment.

## 1.2. Measurement

Several processes interacting with soil moisture, are naturally participating in the water cycle in surface soil layer, which are acquired and considered in the model. Evapotranspiration, infiltration and runoff depend on soil wetness, as does the sensible heat flux from the surface and the heat stored in soils. Soil water controls forcing factors and feedbacks between the subsurface and the atmosphere, thereby giving it a significant role in moderating weather and climate, and in controlling the partitioning between surface runoff and infiltration on one hand, and evapotranspiration on the other. Because of soil moisture's importance for so many different fields, it has received much attention, from theoreticians and modellers and from experimenters and observers. Nevertheless, how soil moisture dynamics behave under the seasonal frozen ground, where dramatic freezing–thawing occurs, is still not fully investigated. To investigate that, one would like to observe liquid soil moisture under frozen condition.

Time-domain reflectometry (TDR) has been widely used to measure unfrozen water content in frozen soil (Hayhoe, Topp, & Bailey, 1983; Spaans & Baker, 1995; Boike & Roth, 1997; Stähli & Stadler, 1997; Flerchinger, Seyfried, & Hardegee, 2006; Watanabe & Wake, 2009; He & Dyck, 2013). However, past studies indicated that unfrozen water in frozen soil measured by TDR is often overestimated when determined by the relationship between soil water content and bulk dielectric permittivity of soil due to the much higher permittivity of ice compared to that of air (Yoshikawa & Overduin, 2005).

The coexistence of water and ice in frozen soils engenders an exclusive situation on hydraulic, thermal and mechanical properties of frozen soils. In order to capture the screen of the state and movement of water in frozen soil, the measurement of both the temperature and the volume of water is needed. And, it is required to quantify the amount of water in different forms- the total amount of water in frozen soil, which is total soil water content (TSWC), and the other two vital variables, liquid soil water content (LSWC) and soil ice content (SIC).

Although there is a tiny amount of water can infiltrate when the soil is frozen, and can generate surface runoff immediately, the vertical movement of water in frozen soil is supposed to be a feedback of freeze–thaw process. Therefore, the infiltration rate may become an indicator for the variation of the freeze–thaw processes, which may be captured by monitoring soil moisture, in another word, LSWC at in-situ. In addition, all the three above-mentioned variables (TSWC, LSWC and SIC) can be simulated by using the land surface model (LSM).

The field determination of SIC is more challenging than that of LSWC or TSWC and no practical method has been found (Cheng et al., 2013). The dominant method to measure the SIC in frozen soil is to measure TSWC and LSWC simultaneously, and then evaluating SIC in a single subtraction. In recent research, there is a trend to have various sensors to measure the TSWC and LSWC, such as gas dilatometry, dielectric spectroscopy, heat pulse probe method.

Nevertheless, the Tibet-Obs (Tibetan Plateau Scale of Soil Moisture and Soil Temperature Observation Network) (Su et al., 2011) provides necessary measurements of soil moisture and soil temperature over a seasonal frozen ground, Maqu, Tibetan Plateau, China, for detecting SIC. Although the direct measurement of SIC is not feasible yet at the Tibet-Obs, the in-situ observed hydrothermal states of the soil will definitely help to investigate the freeze–thaw processes, when combined with model simulation results.

## 2. RESEARCH PROBLEM

### 2.1. Major interests

The overwhelming interests of the study focus on qualifying and representing the freeze-thaw processes in seasonal frozen grounds. The major issue, for this study, is to detect the amount of water at different phases (e.g. TSWC, LSWC & SIC), and to investigate the processes of freeze-thaw transitions in frozen soil. This can be only feasible via LSM modelling and in-situ observations.

It is supposed that the movement of water and the phase transition are presented at soil moisture and soil temperature which may be dominantly affected by soil texture, soil porosity. Therefore, the selected numerical model should help to reveal the relationships between the LSWC, SIC and temperature and other influential factors, and to verify the knowledge of the freeze-thaw processes. In this study, the community Noah land surface model (Ek, 2003) is selected for this purpose.

With the LSM, all the three above-mentioned key variables can be produced. More specifically, the SIC can be determined indirectly from  $SIC = TSWC - LSWC$ . Therefore, the research problem for this study is following:

#### **Can Noah LSM represent accurately the freeze-thaw process over the seasonal frozen ground?**

The task in this study is, therefore, mainly about constructing a long-term simulation of freeze-thaw process by using Noah LSM, precisely as possible to represent the processes at various depths. In addition, the in-situ measurement of LSWC can help to validate the model simulation results (e.g.  $LSWC = TSWC - SIC$ ). For this study, the Maqu network of Tibet-Obs will be deployed for this purpose.

## 3. OBJECTIVES AND QUESTIONS

### 3.1. Objectives

The main objective of this thesis is to use a numerical model to investigate the freeze-thaw processes in seasonal frozen soil, and therefore, better acknowledging the water cycle over the seasonal frozen ground. Accordingly, the sub-objectives and questions are presented in following sub-sections.

### 3.2. Sub-objectives

- To evaluate how accurate it is for the Noah simulation of freeze-thaw process;
- To understand the long-term dynamic of freeze-thaw process over a seasonal frozen area

### 3.3. Research Questions

- Can the Noah simulation results representing the in-situ measurement of soil moisture and soil temperature?
- After all, what is the long-term dynamic of freeze-thaw processes over a seasonal frozen area like Maqu?

## 4. STUDY AREA

### 4.1. Maqu observation station

The remarkable elevation of Tibetan Plateau, average above 3000 m, occupying more than 2.6 million km<sup>2</sup>, plays a vital role in continental or even global climate. The temperature on Tibetan Plateau cycles to reach zero degree for nearly half a year and large range of diurnal variation on surface temperature. Together with barbarian ground with little living creature, and open field, Tibetan Plateau with high altitude provides an ideal field to observe the freezing-thawing process.

On the northeast region of Tibetan Plateau, there is an area, Source Region of Yellow River (SRYR), where temperature generally remains below 0 degree for approximately 5 months a year. The Maqu county, located in the northeast part of SRYR, has a temperature ranging from -4 degree Celsius to 2 degree Celsius. The low temperature provides a dynamic area where the soil annually frozen while October to April, and remains unfrozen at the top on the other half of year (Zheng, Van der Velde, et al., 2015).

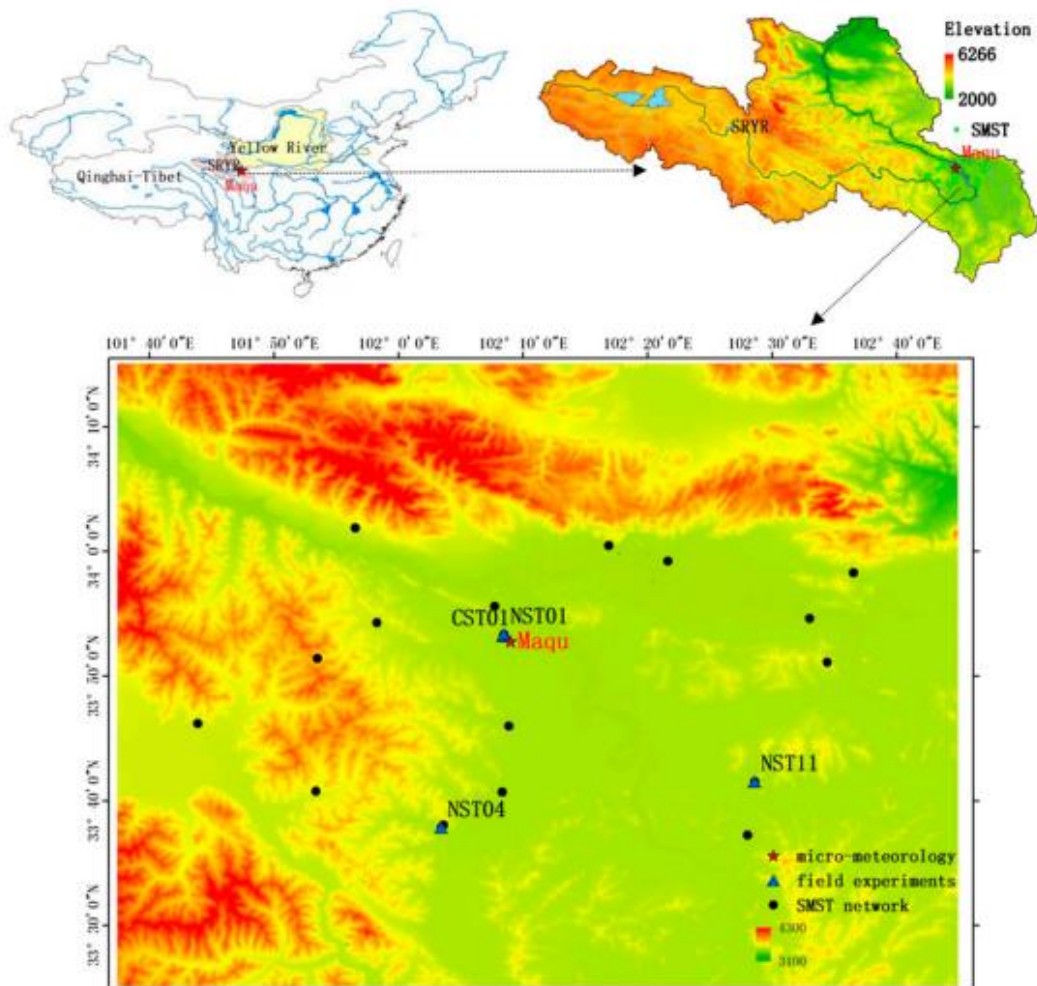


Figure 4.1.1 Location of study area, Maqu, Gansu Province, China<sup>1</sup>

1

<sup>1</sup> Figures from Zheng, D., R. Van der Velde, Z. Su, X. Wang, J. Wen, M. J. Booij, A. Y. Hoekstra, and Y. Chen (2015a), Augmentations to the Noah model physics for application to the Yellow River source area. Part I: Soil water flow, *J. Hydrometeo*, vol. 16(6), 2659–2676.

## 4.2. In-situ Datasets

The comprehensive in-situ datasets include in-situ micro-meteorological and profile soil moisture and soil temperature. Equipment deployed at Maqu station were set up measuring soil moisture (SM), soil temperature (ST) by EC-TM tube of ECH<sub>2</sub>O probe family, and other hydro-meteorological variables. The network of 20 soil moisture and soil temperature (SMST) monitoring sites, covering a region of 40 km by 90 km centred on the micro-meteorological observing system has been setup as a part of the Tibetan Plateau Observatory (Tibet-Obs). All the measurements are processed to values for every 10-min or 15-min interval, and the soil temperature is measure at 5 different depths to the ground, data collected at sites CST series, numbers at five stations, and NST, numbers at 15, are averaged for each soil depth (-0.05, -0.10, -0.20, -0.40, and -0.80 m).

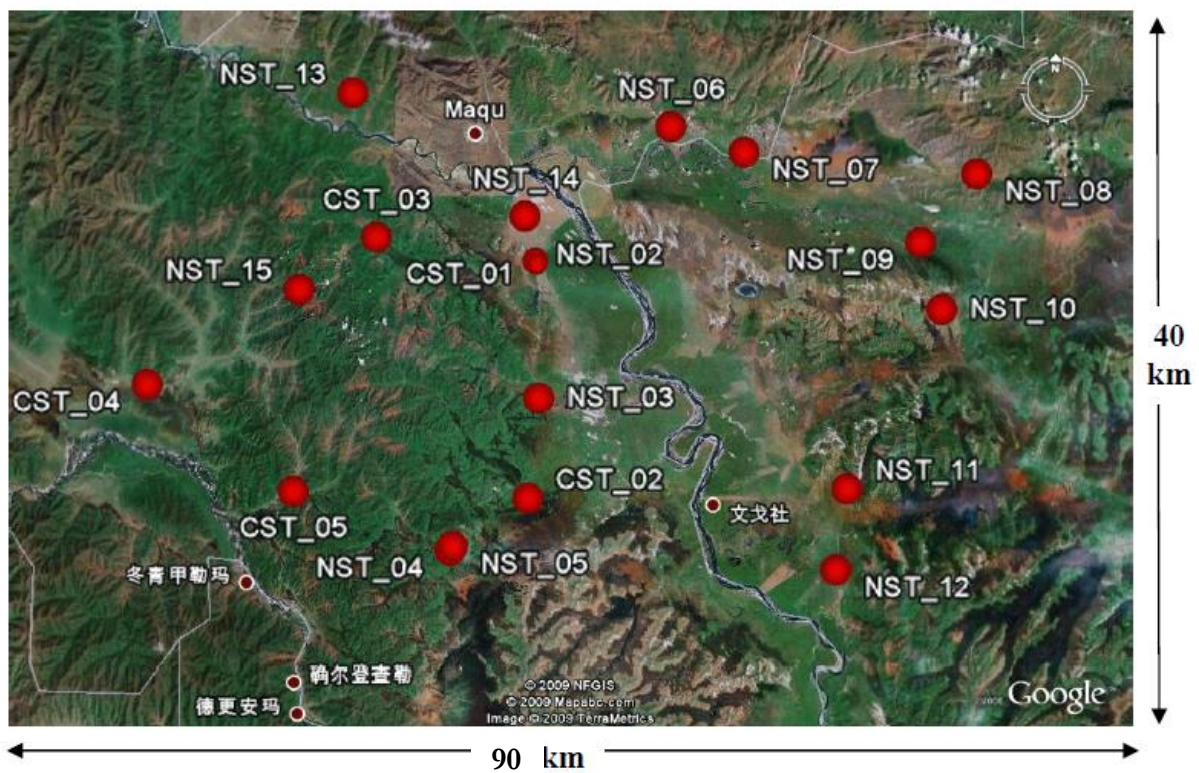


Figure 4.2.1 SRYP Network

## 5. METHODOLOGY

### 5.1. Noah Land Surface Model

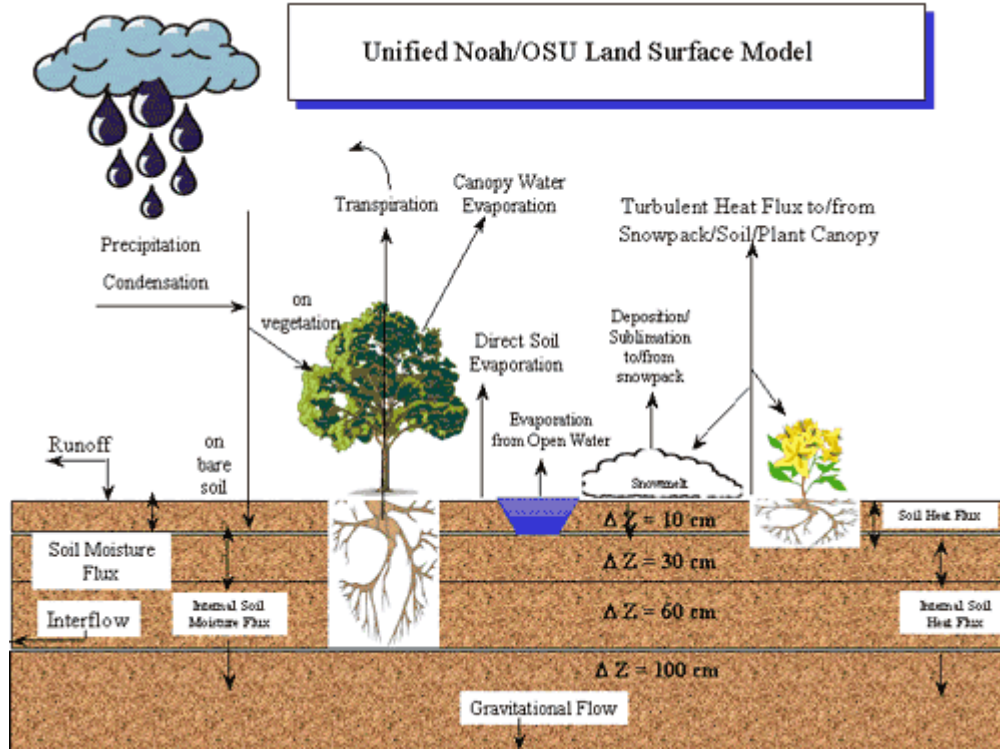


Figure 5.1.1 Noah Land Surface Model <sup>2</sup>

The Noah LSM is selected as the model for the research presented in this thesis. The monitoring system constructed is mainly based on the Noah land surface model (LSM) originated from the Oregon State University (OSU). A four-layer soil scheme is implemented with the thermal diffusion equation for simulating heat transport and diffusivity form of Richards' equation for water flow (Mahrt & Pan, 1984; Pan & Mahrt, 1987). A simple water balance approach (Schaake, et al. 1996) is adopted to simulate the surface runoff and the cold season physics are implemented as described in Koren et al. (1999).

#### 5.1.1. Soil heat flow

In unfrozen soils, heat vertically migrates following the steps of heat flux.

$$C_s \frac{\partial T}{\partial t} = \frac{\partial}{\partial z} (\kappa_h \frac{\partial T}{\partial z}) \quad (5.1.1)$$

where  $\kappa_h$  is the thermal heat conductivity ( $\text{W}\cdot\text{m}^{-1}\cdot\text{K}^{-1}$ ), and  $C_s$  is the thermal heat capacity ( $\text{J}\cdot\text{m}^{-3}\cdot\text{K}^{-1}$ ).

The solution to eq (5.1) is achieved using the fully implicit Crank-Nicholson scheme. The temperature at the bottom boundary (at a depth of 8 m below the ground surface) is generally taken as the annual mean near-surface air temperature, whereas the top boundary at 0 m from the surface is confined by surface temperature of the ground.

<sup>2</sup> <https://www.ra.lucar.edu/research/land/technology/lsm.php>

### 5.1.2. Soil thermal parameterization

The heat flow through the soil column is parameterized by the thermal heat conductivity and capacity, which depend on constituents of the soil matrix. The thermal heat capacity is calculated using the following equation:

$$C_s = \theta C_{water} + (1 - \theta_s) C_{soil} + (\theta_s - \theta) C_{air} \quad (5.1.2)$$

where  $\theta$  is the soil moisture content ( $\text{m}^3 \cdot \text{m}^{-3}$ ),  $\theta_s$  is the porosity ( $\text{m}^3 \cdot \text{m}^{-3}$ ),  $C_{soil}$ ,  $C_{air}$ , and  $C_{water}$  are refer to heat capacity of soil, air and water, which values respectively at  $2.0 \times 10^6 \text{ J} \cdot \text{m}^{-3} \cdot \text{K}^{-1}$ ,  $1005 \text{ J} \cdot \text{m}^{-3} \cdot \text{K}^{-1}$ ,  $4.2 \times 10^6 \text{ J} \cdot \text{m}^{-3} \cdot \text{K}^{-1}$ .

### 5.1.3. Richards' equation

The diffusivity form of Richards' equation is utilized by the Noah LSM for the simulation of soil water flow, which can be formulated as:

$$\frac{\partial \theta}{\partial t} = \frac{\partial}{\partial z} \left( D(\theta) \frac{\partial \theta}{\partial z} \right) + \frac{\partial K(\theta)}{\partial z} + S(\theta) \quad (5.1.3)$$

Where  $\theta$  is the total soil water content ( $\text{m}^3 \cdot \text{m}^{-3}$ ),  $t$  is time (s),  $D$  is the soil water diffusivity ( $\text{m}^2 \cdot \text{s}^{-1}$ ),  $K$  is the hydraulic conductivity ( $\text{m} \cdot \text{s}^{-1}$ ),  $z$  is the soil depth (m),  $S$  represents sources and sinks (precipitation and evapotranspiration,  $\text{m} \cdot \text{s}^{-1}$ ).

### 5.1.4. Surface water budget

$$\frac{\partial W}{\partial t} = \begin{cases} P - ET_a - R, & ET_p > 0 \\ P - ET_p - R, & ET_p \leq 0 \end{cases} \quad (5.1.4)$$

Where  $\frac{\partial W}{\partial t}$  is the change in water storage (m),  $P$  is the total precipitation (m),  $ET_p$  is the potential evapotranspiration (m),  $ET_a$  is the actual evapotranspiration (m), and  $R$  is the total runoff (m) all within a model time step. The second case in above equation represents the condition when the dew forms.

## 5.2. Noah LSM: Freeze-thaw process

To account for soil moisture phase change during freeze-thaw transitions, a source term is added to the thermal diffusion equation as Koren et al. (1999):

$$C_s(\theta, \theta_{ice}) \frac{\partial T}{\partial t} = \frac{\partial}{\partial z} \left( \kappa_h(\theta, \theta_{ice}) \frac{\partial}{\partial z} \right) + \rho_{ice} L_f \frac{\partial \theta_{ice}}{\partial t} \quad (5.2.1)$$

Where  $\rho_{ice}$  is the density of ice ( $\text{kg} \cdot \text{m}^{-3}$ ),  $L_f$  is the latent heat of fusion ( $\text{J} \cdot \text{kg}^{-1}$ ),  $\theta$  is the total soil water content ( $\text{m}^3 \cdot \text{m}^{-3}$ ),  $\theta_{ice}$  is the soil ice content ( $\text{m}^3 \cdot \text{m}^{-3}$ ). The heat source term is determined by the soil water phase equilibrium estimated using the water potential- freezing point depression equation as well as the available heat (Koren et al. 1999). The thermal parameterization is modified to consider the effect of ice content as in Peters-Lidard et al. (1998).

With the assumption that liquid water flow in the frozen soil is analogous to that in unfrozen soil, the diffusivity form of Richards' equation can be also adopted to estimate movement of liquid water:

$$\frac{\partial \theta_{liq}}{\partial t} = \frac{\partial}{\partial z} \left( D(\theta_{liq}) \frac{\partial \theta_{liq}}{\partial z} \right) + \frac{\partial K(\theta_{liq})}{\partial z} + S(\theta) \quad (5.2.2)$$

Where  $\theta_{liq}$  is liquid soil water content ( $\text{m}^3 \cdot \text{m}^{-3}$ ),  $t$  is time (s),  $D$  is the soil water diffusivity ( $\text{m}^2 \cdot \text{s}^{-1}$ ),  $K$  is the hydraulic conductivity ( $\text{m} \cdot \text{s}^{-1}$ ),  $t$  is the time,  $D$  is the soil water diffusivity,  $K$  is the hydraulic conductivity,  $S$  represents sources and sinks such as precipitation and evapotranspiration.

### 5.3. ECH<sub>2</sub>O probe

For the current proposed laboratory experiment, ECH<sub>2</sub>O capacity tube is widely applied to determine the SIC. The inter-comparison of the results will help to identify how effective the ECH<sub>2</sub>O family of sensors can monitor LSWC under frozen condition. And if possible, the proposed laboratory experiment can help to develop a semi empirical approach for determining the SIC directly from the ECH<sub>2</sub>O sensors. The sensor types include EC-10, EC-TM and 5TM. The ECH<sub>2</sub>O family of sensors measures the LSWC using a capacitance technique. By rapidly charging and discharging a positive and ground electrode (capacitor) in the soil, an electromagnetic field is generated whose charge time is related to the capacitance (C) of the soil.

To determine the liquid water content, the 5TM probes we've settled, designed by Decagon Device Incorporation, use an oscillator running at 70 MHz to measure the dielectric permittivity of soil. And a thermistor in thermal contact with the sensor prongs provides the soil temperature capable to detect the temperature range from -40 °C to 60 °C.

### 5.4. Flowchart

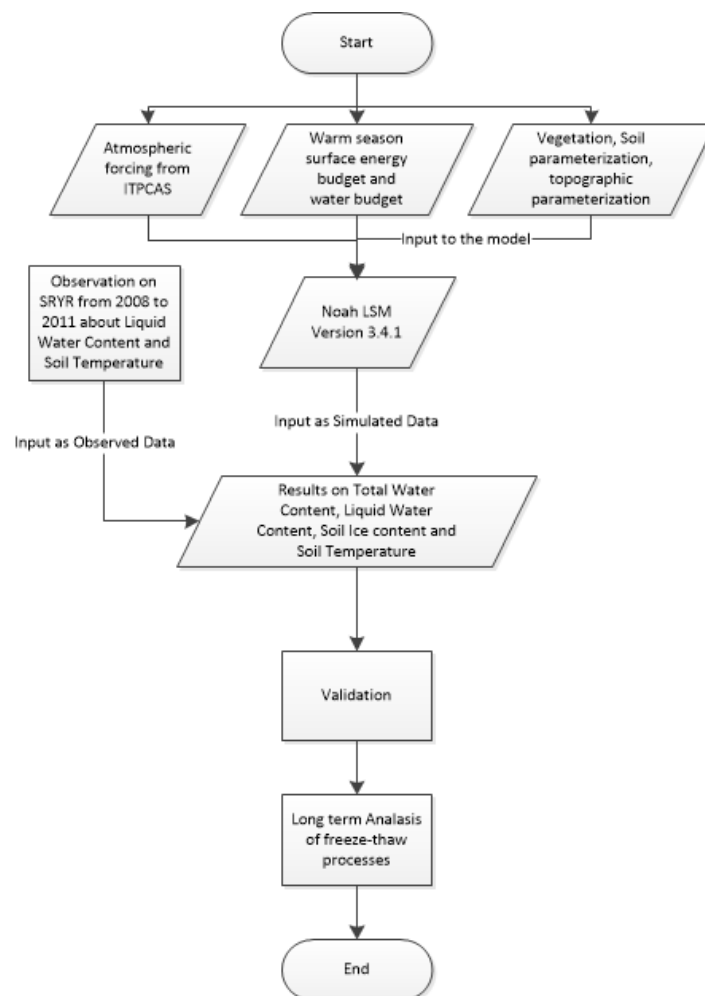


Figure 5.4.1 Flowchart

The figure above is the flowchart which contains the description of the main progress implemented on this thesis. The overriding concern on this thesis is measuring the precise amount SIC at long term period to

understand the dynamic behaviour of it. When measuring the SIC, it is taken to use an indirect way since the data source is deducible that it is available to study the behaviour of SIC.

First of all, the source data is composed of simulated data and observed data. The previous one was retrieved from Noah LSM which is built up and validated specially on the SRYR by Donghai (Zheng, 2015). The model simulation results from Zheng (Zheng, van der Velde, et al., 2015) were used directly in this study. And the observation from Maqu monitoring network installed in May and June of 2008 offers a three-year observation on SM/ST at 10, 15 minutes interval, at 5 different depths (5 cm, 10 cm, 20 cm, 40 cm, 80 cm). Since the simulation results are at a different format at depth of 4 layers, (5 cm, 25 cm, 70 cm, 160 cm), it is required to bring it in lines with the observed data both by depth and by intervals before validation. Referred to the simulation data, the reshaping process on observation data includes an interpolation at depth and an extraction for time series from July 1<sup>st</sup>, 2008 till June 30<sup>th</sup>, 2009. The last part of preparation step is to obtain coordinates from the observation data and to match them to the corresponding simulated pixels from the 4\*9 array at the interest area of SRYR.

Root mean square error (RMSE) and correlation coefficient ( $R^2$ ) is selected to present the quality of validation applied on different layers respectively. The results contain a portion of null for the observation data is not available at certain period and also at certain depth.

Thirdly, a long-term analysis of the simulation results was carried out on freeze-thaw processes. The results analysis focuses on the behaviour of the four variables from simulation results, LSWC, SIC, TSWC, and ST, at long term variation, especially on SIC. Both the longest continuous duration of valid ice and lag time between different layers are introducing the images of the freeze-thaw process at SRYR. . Since the soil temperature is overestimated at winter, valid icing days are calculated by the constraint ( $ST < 0$ ). Last but not least, the Active Layer Thickness (ALT), an indicator of the movement of ice in soil, is produced by constraining  $SIC > 0.004$ , and  $ST < 0$  from the simulation results.

## 6. VALIDATION RESULTS AND ANALYSIS

### 6.1. Validation results

#### 6.1.1. Pixel-wise process

According to the original simulation results, the water cycle at the interesting area in SRYR at is modelled as 4\*9 pixels domain, the location of each observation station is shown in the picture below.

		NST13			NST06	NST07		NST08
	NST15	CST03	NST14	CST01 NST01 NST02				NST09 NST10
CST04				NST03				
	CST05		NST04 NST05	CST02			NST11 NST12	

Figure 6.1.1 Simulation and Network

Grouped up by 13 different pixels among the 36 (4 rows and 9 column), only the pixels, size at 10 square kilometres, where the observations stations locates are involved at validation process. Orange pixels are that have only one station on it and the red pixels have multiple stations which required combination, and the rest in yellow represent that there is no station on them.

#### 6.1.2. Validation process

During validation, there are two main difficulties to be solved. One is the bizarre records (e.g. sometime 10min interval, sometime 15min interval and sometime no normal records), and the other is that the record introduced a complex situation in terms of the observation layers in different pixels (e.g. different pixel has different observation depths and difficult to be combined in those red pixels shown in Figure 6.2).

The bizarre records can be caused by battery dysfunction due to low temperature. Despite of the errors, quality check in the data can help to pick out those bad records. These bad records will be removed from the validation processes, assuming that the apparatus were out of energy or dysfunction somehow by the severe weather. This happened in several stations, NST01, NST02, and CST04, the solution is in two steps. Firstly, if the data are in good shape and last for more than 10 months, it is suggested to get rid of the gaps and jumps in order to extract the valid data for analysis. Secondly, if the data are in bad shape and less than 3 months continuous observation, it is judged invalid and would be removed from the validation processes.

The second difficulties are the mixing valid observation layer of different stations. The most crowded pixel is at row 3, column 5, where the central of Maqu county is exactly located. Unfortunately the station CST04, NST01 and NST02 were not producing available data in 2008-2009 periods due to some unknown reasons,

so the number of involved stations in validation process is reduced to 17. These observations at uneven layering were interpolated by inverse distance weight (IDW) into three layers (0.05, 0.25, 0.70 m).

## 6.2. Statistic results

The table below presents the statistical numbers: root mean square error for the comparison of observation and simulation data for all the stations in Maqu network, between July 1<sup>st</sup>, 2008 and June 30<sup>th</sup>, 2009 at 30 minutes interval.

$$RMSE = \sqrt{\frac{1}{n} \sum_{i=1}^n (x_{obs,t,d} - x_{sim,t,d})^2} \quad (6.2.1)$$

$$R^2 = 1 - \frac{\frac{1}{n} \sum_{i=1}^n (x_{obs,t,d} - x_{sim,t,d})^2}{\frac{1}{n} \sum_{i=1}^n (x_{obs,t,d} - \bar{x}_{obs})^2} \quad (6.2.2)$$

Where  $n$  is the index number of the data,  $x_{obs,t,d}$   $x_{sim,t,d}$  stands for the observation data and simulated data at certain time  $t$  and at certain layer  $d$ .

### 6.2.1. RMSE

First of all, the absolute value of RMSE (Root mean square error) of soil moisture, range between 0.07 and 0.23 m<sup>3</sup> m<sup>-3</sup>, while soil temperature from 1.08 to 5.83 degrees. The deeper layer has smaller RMSE (e.g. for both SM and ST), which means the simulated SMST having smaller fluctuations at deeper depth as the dynamics of SMST is damping with increasing depth. For instance, the RMSE of pixel, row 1, column 5 (CST02), are 3.93, 2.32, 1.80 from the first layer to the third layer at soil temperature, and 0.15, 0.08, 0.04 m<sup>3</sup> m<sup>-3</sup> in soil moisture at the same sequence.

**Table 6.2.1 RMSE for the validation of Noah simulation over Maqu Network**

Station	row	column	Pixel Number	SM	ST	SM	ST	SM	ST
				1stlayer 5cm	1stlayer 5cm	2ndlayer 25cm	2ndlayer 25cm	3rdlayer 70cm	3rdlayer 70cm
CST05	1	2	1	0.075369	4.373188	0.055733	1.425186	0.039032	1.549475
NST04 NST05	1	4	2	0.137644	4.553783	Null	Null	Null	Null
CST02	1	5	3	0.122246	3.936791	0.091133	2.245094	0.095233	1.996759
NST11 NST12	1	8	4	0.079869	5.314863	Null	Null	Null	Null
CST04	2	1	Null	Null	Null	Null	Null	Null	Null
NST03	2	5	5	0.087329	5.187282	0.090520	2.040740	Null	Null
NST15	3	2	6	0.139001	4.090368	Null	Null	Null	Null
CST03	3	3	7	0.148434	4.483645	0.075712	1.409164	0.035326	1.258506
NST14	3	4	8	0.069571	5.121007	Null	Null	Null	Null
CST01	3	5	9	0.087869	5.102171	0.064638	1.771688	0.097950	1.082854
NST01 NST02	3	5	Null	Null	Null	Null	Null	Null	Null
NST09 NST10	3	9	10	0.106931	5.297301	Null	Null	Null	Null
NST13	4	3	11	0.10372	4.821948	Null	Null	Null	Null
NST06	4	6	12	0.125992	5.836425	0.046385	1.954745	Null	Null
NST07	4	7	13	0.103988	5.186912	Null	Null	Null	Null
NST08	4	9	14	0.231126	4.635571	Null	Null	Null	Null

### 6.2.2. R<sup>2</sup>

The lumped pixels with multiple stations have lower accuracy than the pixels with single one. This may results from the combined method applied by multiple stations, which introduces uncertainty lowering the accuracy.

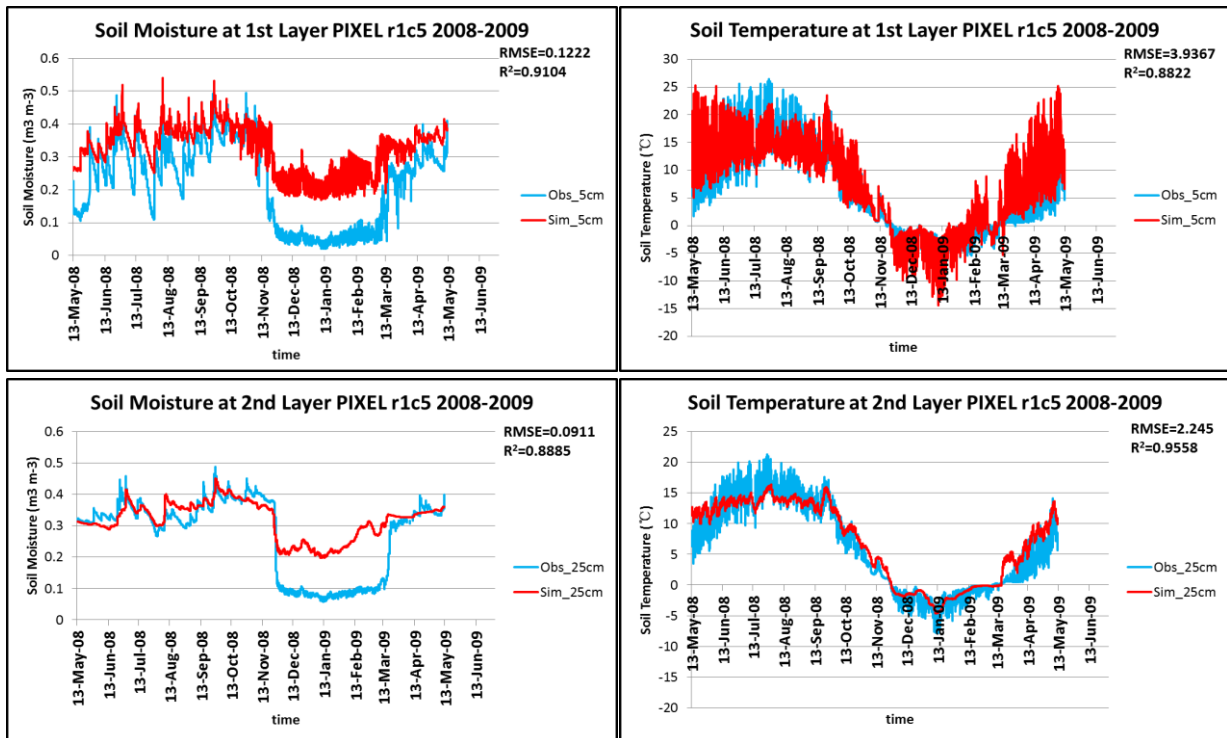
According to the table 6.2, the numbers of correlation coefficient are popular between 0.8 and 0.9. Some reach as high as 0.99, which suggests that the model is perfect performance in simulating the third layer of soil temperature at the pixel locates at row 1 column 2 where the CST05 is involved. At the same time the lowest value touch the bottom at 0.58 at station CST02 in pixel, row 1 column 5. For the others, the appearance of correlation coefficient give rise to an assumption that there is a firm relation between observed data and simulated data both soil moisture and soil temperature.

However, the results of SM and ST validation show slightly different results. When separately zooming into the two variables, the correlation coefficient on soil moisture is higher than that of soil temperature at the first layer but lower in the lower layers, which means the accuracy of the simulation has better performance at soil moisture than soil temperature at the first layer, but poor performance of soil moisture than soil temperature at the lower two layers.

**Table 6.2.2 Correlation coefficients for the validation of Noah simulation over Maqu Network**

Station	row	column	Pixel Number	SM	ST	SM	ST	SM	ST
				1stlayer 5cm	1stlayer 5cm	2ndlayer 25cm	2ndlayer 25cm	3rdlayer 70cm	3rdlayer 70cm
CST05	1	2	1	0.859638	0.806353	0.915278	0.970211	0.847728	0.990071
NST04	1	4	2	0.782225	0.796107	Null	Null	Null	Null
NST05									
CST02	1	5	3	0.910498	0.882293	0.888512	0.955881	0.84541	0.964313
NST11	1	8	4	0.831526	0.800693	Null	Null	Null	Null
NST12	1								
CST04	2	1	Null	Null	Null	Null	Null	Null	Null
NST03	2	5	5	0.860545	0.785111	0.903659	0.956725	Null	Null
NST15	3	2	6	0.905986	0.838651	Null	Null	Null	Null
CST03	3	3	7	0.899724	0.824018	0.944249	0.967374	0.883234	0.984453
NST14	3	4	8	0.890042	0.778326	Null	Null	Null	Null
CST01	3	5	9	0.811481	0.798378	0.844147	0.966862	0.842956	0.984998
NST01	3	5	Null	Null	Null	Null	Null	Null	Null
NST02	3	5	Null	Null	Null	Null	Null	Null	Null
NST09	3	9	10	0.744386	0.792777	Null	Null	Null	Null
NST10	3								
NST13	4	3	11	0.851831	0.806482	Null	Null	Null	Null
NST06	4	6	12	0.80383	0.751955	0.89841	0.963641	Null	Null
NST07	4	7	13	0.83736	0.798587	Null	Null	Null	Null
NST08	4	9	14	0.809984	0.833699	Null	Null	Null	Null

### 6.3. Validation results analysis



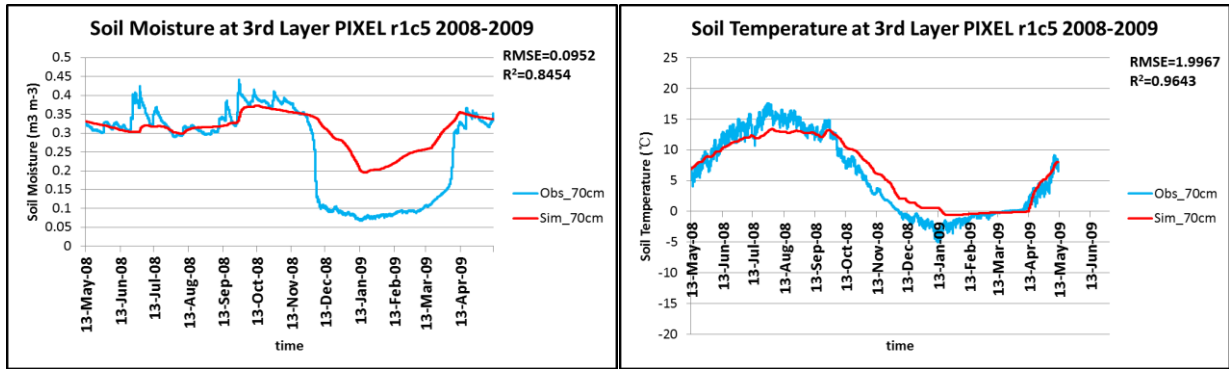


Figure 6.3.1 Validation results on Station CST02 (ROW 1 COLUMN 5)

The simulation on SM and ST are reliable according to not only on the statistic numbers but also figures. For example, on station CST 02, which provides a nearly 12-month long observation data, pigments in blue, observation records are fully available for the top three layers. Simulated results are pigment in red, and are comparably pictured with the 2 variables at the 3 different layers (Figure 6.3.1).

During winter period(November till March), the simulation result as overestimated the soil moisture (e.g. Simulated\_SM – Observed\_SM), in terms of average value, of 0.1, 0.15, 0.18m<sup>3</sup> m<sup>-3</sup> from 1<sup>st</sup> layer to 3<sup>rd</sup>layer, respectively. However, the underestimation can be seen over the rest of seasons. The simulation underestimates observation around 0.1m<sup>3</sup> m<sup>-3</sup>from April till October. For soil temperature, the simulated soil temperature underestimates observation during winter for the top layer, while overestimate for the 2<sup>nd</sup> and 3<sup>rd</sup> layer.

In spite of the accuracy of values, also the lag time between different layers has various performances. The beginning of diving of lines in winter on soil moisture at first layer is matching on time but underestimated the deepness it can reach to. The other layers have mistakenly assessed on the timing it drops, roughly 10 days in advance on 2<sup>nd</sup> layer and 30 days at 3<sup>rd</sup> layer. These results are introducing a rethink on the model about the underestimates on soil moisture in winter period at the relatively higher temperature, and the SIC. The lag time is not prominent on figures of soil temperature for the first two layers, and the greatest gaps among the 3 figures, shown at 3<sup>rd</sup> layer is less than 4 days.

#### 6.4. Conclusion of validation

This study suggests that the observation at field across the soil profile provides a reliable simulation in soil temperature and soil moisture for the validation of Noah LSM. For most of the simulation results on soil moisture, the lines are greater fluctuant at short variations, but are less variable to the long term period which cannot match the observation data. During winter period, they present a significant overestimation on all three layers, especially the first layer which suggests the lower accuracy on it. Because the complex water movement and phase change happened at higher frequency at this most active layer.

However, unparalleled to the poor precision of soil moisture, simulations on soil temperature have better performance. On both layers, it is illustrated from the figure 6.3 that simulation results of the soil temperature have higher accuracy than soil moisture in all three layers. Both figures from soil temperature have insignificant time lag, consistent variation, and small deviation which the soil moisture groups fail to show up. These validation figures and numbers reveal that the validation results are excellent and the model

is good enough to produce a relatively simulation results for further study about the water processes. However, to some extent the results give rise to at least two suggestions.

In the appendix, please see all the validation results for each station, each pixel collocated with corresponding stations, and for the whole Maqu network represented by an average.

## 7. SIMULATION RESULTS AND ANALYSIS

### 7.1. Soil moisture and soil temperature

#### 7.1.1. Total results and analysis

**Table 7.1.1 Simulation results between different layers**

Variables		1stLayer	2ndLayer	3rdLayer	4thLayer
LSWC (m <sup>3</sup> m <sup>-3</sup> )	average	0.309755	0.310392	0.30076	0.334547
	st.dev	0.084405	0.074802	0.06394	0.038357
SIC (m <sup>3</sup> m <sup>-3</sup> )	average	0.053345	0.047232	0.040022	0.011955
	st.dev	0.078865	0.074586	0.06057	0.018442
TSWC (m <sup>3</sup> m <sup>-3</sup> )	average	0.3631	0.357624	0.340781	0.346502
	st.dev	0.057818	0.038172	0.031788	0.028543
ST (°C)	average	6.053085	5.828117	5.551388	5.272007
	st.dev	8.211872	6.616868	5.195857	4.294989

The total amount of water is higher at the close part of surface and lower at the bottom layer. It is similar for the liquid water contents when compared to that of TSWC for the first three layers, but reaching the greatest amount of liquid water at the fourth layer. The SIC on the fourth layer is only about 20% of that of first layer. It suggests that although it has lower average temperature, the bottom layer produce less ice than the sensitive and active first layer. The first layer produces almost 4 times ice greater than the fourth layer. Standard deviation of ST also drops from top to bottom, which suggest the deeper layer are more stable at temperature.

**Table 7.1.2 LSWC and SIC Percentage of Simulation results between different layers**

	1stLayer	2ndLayer	3rdLayer	4thLayer
LSWC(TOTAL)	85.50%	87.03%	88.38%	96.53%
SIC(TOTAL)	14.47%	12.95%	11.60%	3.43%
LSWC(WINTER)	63.83%	67.63%	71.00%	91.43%
SIC(WINTER)	36.18%	32.38%	29.00%	8.58%

For most of the year, the liquid water takes up 99 % the total amount of water, and for winter season, the SIC climb up to approximately 2.5 times as yearly average since the long lasting period of SIC.

Moreover, the simulation results are classified into 4 smooth types, 1 day average, 3 day average, 7 day average, and 1 month average in order to understand the behaviour of simulation. As will be discussed in the following, the half-hourly simulation is the most suitable for the current study on the freezing/thawing process. Nevertheless, those results are shown in the appendix.

### 7.1.2. Total Water Content

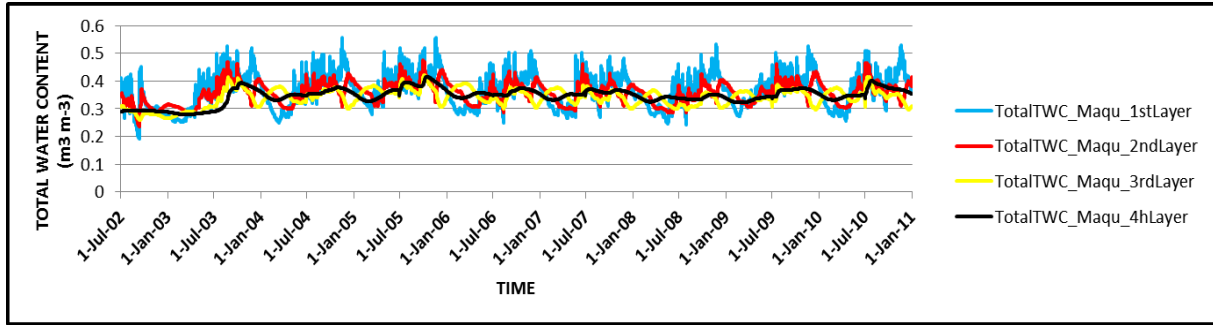


Figure 7.1.1 Simulation Results-TSWC

For the total water content, it fluctuates frequently at the first layer since it is more active layer where there have intensive frequencies of water movement of the evapotranspiration, infiltration and capillary rising. The soil moisture of first layers gradually climbs up in the mid February and peak at value of 0.50 at the beginning of every July, which is almost summit for the four layers can achieve. Followed by several waves, the curve immediately dive after reaching the last peak at around 1st October. When bottom at approximately 0.15 during first half of January, the curve do not bounce until February comes. The daily average amount in first layer is lowest of the four, estimated as approximately  $0.3103 \text{ m}^3 \text{ m}^{-3}$  per day, and the deeper layers are likely to contain much water and therefore less affected by land surface. The fourth layer has as high as  $0.3347 \text{ m}^3 \text{ m}^{-3}$  per day in soil moisture.

The performances of first two layers are loyal twins, which are too close at looking and hardly can be distinguished. They are 90 percent are at similarity not only by the amounts of soil moisture but also by the growing speed of them. The only difference between the twins is that the first layer jumps a little higher and falls deeper since it is the shallowest layer which easily influenced by event caused by atmosphere. And it indicates that the lag between first two layers is tiny for the most period, which induce the idea that the first two layers are similar in every aspect of property and only diversified in response to the rain fall and evapotranspiration.

The trend line of third layers is smoother than the first two but not as flat as the fourth one. The lag is clearly visible. It can be draw as a conclusion that the deeper layers tend to emerges less frequency of fluctuations but higher amount of storage where the greatest amount of soil moisture happens at 4th layer, sway between 0.3 and 0.4 all the time but amount at around  $0.334409216 \text{ m}^3 \text{ m}^{-3}$  per day.

The lag from top layer to bottom layer is increasing from 3 days, 45 days to 90 days. The gap between 3rd layer and 4th layer is tremendous at around 3 months which suggests the depth is a long distance, 110 cm, for the vertical movement of water and heat to transfer during the frozen period. And the unfrozen soil deep into the fourth layer is regard as a heat container and is hard to be influenced by ground.

### 7.1.3. Soil temperature

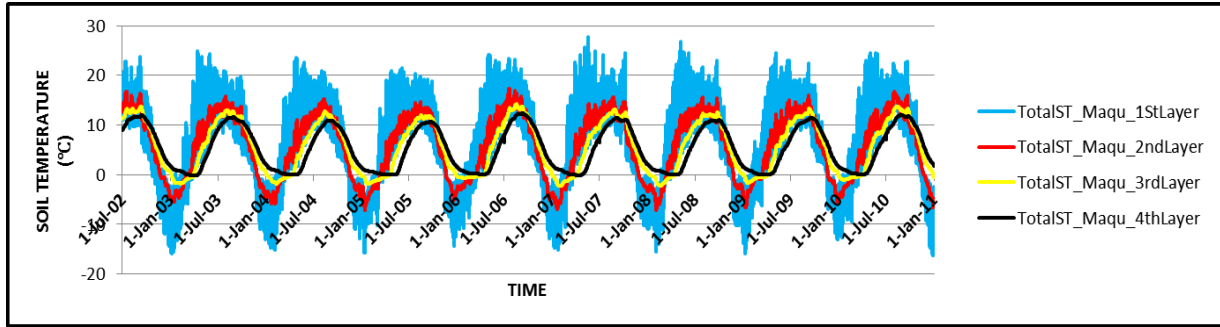


Figure 7.1.2 Simulation Results-ST

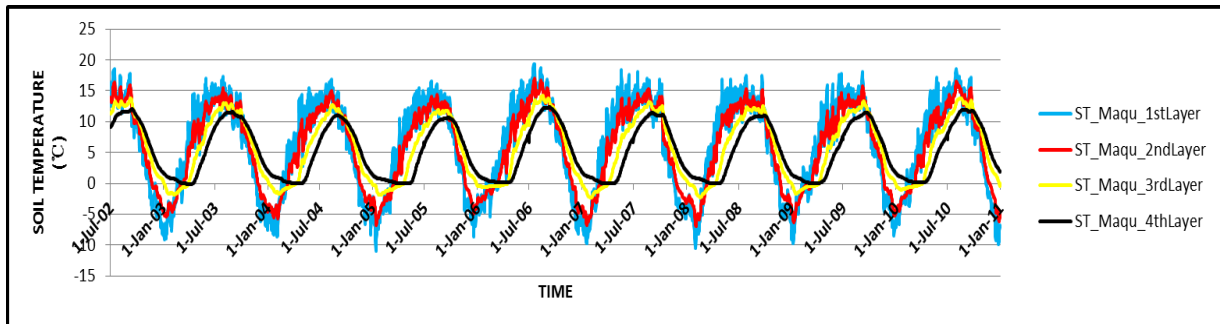


Figure 7.1.3 Simulation Results -ST(Daily Average)

The average temperature is higher at the layers closer to surface than lower layers. The variation of soil temperature remains constant from the figure, and the fluctuation declines from top layer to bottom layer. It ranges from 28 degree Celsius to -15 degree Celsius at the top layer at 5 cm depth, and the range narrows to 12 to -0.5 degree Celsius at the bottom layer, depth at 160 cm. What the figures are presenting is sensitive and dynamic layer on the top and insensitive and inertia at the bottom for the reason that ground surface is modelled as source pool of heat. Moreover, it seems to have too less negative numbers and lower temperature at deeper layer which prevents it from producing enough SIC.

Table 7.1.3 Minimum value and its date of Soil temperature

YEAR	1stLayer	2ndLayer	3rdLayer	4thLayer
2002-2003	5-Jan-03	12-Jan-03	9-Feb-03	10-Apr-03
2003-2004	2-Feb-04	6-Feb-04	10-Feb-04	15-Apr-04
2004-2005	12-Jan-05	14-Jan-05	28-Jan-05	22-Apr-05
2005-2006	20-Dec-05	21-Dec-05	1-Feb-06	14-Apr-06
2006-2007	18-Jan-07	18-Jan-07	2-Feb-07	8-Apr-07
2007-2008	2-Feb-08	3-Feb-08	18-Feb-08	14-Apr-08
2008-2009	7-Jan-09	10-Jan-09	18-Jan-09	4-Apr-09
2009-2010	25-Dec-09	26-Dec-09	19-Jan-10	31-Mar-10
<b>AVERAGE</b>	<b>11-Jan</b>	<b>13-Jan</b>	<b>1-Feb</b>	<b>10-Apr</b>

The table above reveals the day when the respective layer get to the lowest temperature of 8 cycling period. The minimum temperature of 1<sup>st</sup> layer occurs around 11<sup>th</sup> January, and the second layer has 2 days lag time.

The soil temperature will climb up soon after reaching the bottom from the first two layers, but by the same time the bottom layer has decreasing temperature till April. This lag time is representative of the shape of wave of ST and their discrepancies on different layers. Also, it is expectedly similar to that of SIC since the ice will come up with response to the low temperature.

**Table 7.1.4 Lag time between different layers of Minimum value and its date of Soil temperature**

YEAR	Lag1_2	Lag2_3	Lag3_4
2002-2003	7	28	60
2003-2004	4	4	65
2004-2005	2	14	84
2005-2006	1	42	72
2006-2007	0	15	65
2007-2008	1	15	56
2008-2009	3	8	76
2009-2010	1	24	71
<b>AVERAGE</b>	<b>2.375</b>	<b>18.75</b>	<b>68.625</b>

The lag time between the first two layers is nearly 2 days, but the number increases to 18.75 and 68.625 days at the deeper parts of soil. Since the lag time between the third layer and fourth layer is averagely more than two months. This long lag time represent the heat exchange between different layers it may enormously influence on the formation or thawing of SIC.

## 7.2. Liquid Water Content

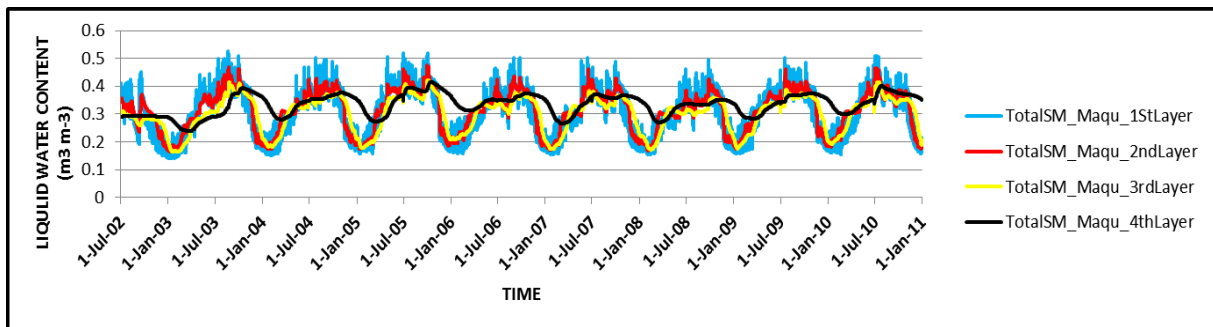


**Figure 7.2.1 Simulation Results-LSWC**

The figures of liquid water content (LSWC) are parallel to the total water content (TSWC) in the monsoon season since LSWC is the only component of the season. However, the lines shape differently in the cold season because of the fact that SIC annually takes up for more than 60 percent of TSWC for most of the period. The peaks of the top three layers of LSWC annually appear at similar period of the year of TSWC, first one at the beginning of July, then several concentrated between August and October, and last but greatest at November. These rapid climbing lines, due to seasonal rainfall are following with quick drops and evapotranspiration. Unlike the variation of peaks, the bottoms from different runs more stable recurs at early February, which suggests dry and cold period, and they remain low till April when monsoon comes with clouds.

### 7.3. Soil ice content

#### 7.3.1. Valid numbers of SIC

**Table 7.3.1 SIC valid days and percentage based on Different threshold**

SIC(0.004Threshold)	SIC_1stLayer	SIC_2ndLayer	SIC_3rdLayer	SIC_4thLayer
valid days	1422	1084	1227	1206
Percentage of year	45.82%	34.93%	39.54%	38.84%
Average days per year	167.34	127.57	144.38	141.83
SIC(0.01 Threshold)	SIC_1stLayer	SIC_2ndLayer	SIC_3rdLayer	SIC_4thLayer
valid Days	1321	1033	1142	1024
Percentage of year	42.56%	33.29%	36.80%	32.97%
Average days per year	155.42	121.56	134.37	120.41

Table 7.3.1 illustrate that in the 8.5 round cycle, the days with valid SIC takes up to 45.82%, more than 167 days per year at average. But this number actually drops to 28.02%, 102.23 days per year when the soil temperature constraint was activated (Table 7.3.2). Further researches need to be carried out to find out why Noah LSM can produce SIC at temperature higher than the freezing point.

A threshold is needed for eliminating the tiny SIC from simulation results as a filter. This threshold is crucial to answer the questions of the quantity of SIC, and the duration of SIC. Threshold is selected at both 0.01 and 0.004  $m^3 \cdot m^{-3}$ , to see what is the discrepancy. The table 7.3.1 illustrates that lower value of threshold has higher numbers of valid days. The first layer is nearly 10% reduced if the threshold rises from 0.004 up to 0.01 at 1<sup>st</sup> layer. And a conclusion can be drawn that a reasonable threshold for valid SIC is 0.004. The numbers of days where soil temperature at 1<sup>st</sup> layer under 0 degrees should not be more than half year at the freezing cycle since the yearly average temperature is around 6 degree at the top layer. So the percentage result, thresholds at 0.004, reaching an astonishing 45.82% is not reasonable and reveals the overestimate on the duration of soil ice at first layer. However, this simulation results suggest a more dynamic freezing and melting processes, for threshold at 0.004 gives better performances at variation of SIC.

Despite of the tiny SIC impeding the analysis, the model also produces anomaly that SIC occurs at warm days reaching a positive temperature which is not valid and should be filtered out from analysis. The anomaly, based on the simulation results from both overestimation at summer and underestimation at winter at soil temperature, seems indicating there is certain drawback in the parameterization of the freezing/thawing process in the Noah LSM. The solution is to establish a constraint on the temperature, to reduce the wrong calculation of SIC.

**Table 7.3.2 Valid SIC days and percentage of the simulation results (cycle based)**

Days	Total		Daily Average		Percentage of cycle	Total		Daily Average	
	SIC>0.004	ST<0	SIC>0.004	ST<0		SIC>0.004	ST<0	SIC>0.004	ST<0
1st Layer	167.34	102.13	190.82	101.88	1st Layer	45.82%	27.97%	52.26%	27.90%
2nd Layer	127.57	106.63	127.76	106.71	2nd Layer	34.93%	29.20%	34.99%	29.22%
3rd Layer	144.38	91.64	144.82	91.76	3rd Layer	39.54%	25.10%	39.66%	25.13%
4th Layer	141.83	15.43	142.00	15.41	4th Layer	38.84%	4.22%	38.89%	4.22%

### 7.3.2. Long term variation and Duration

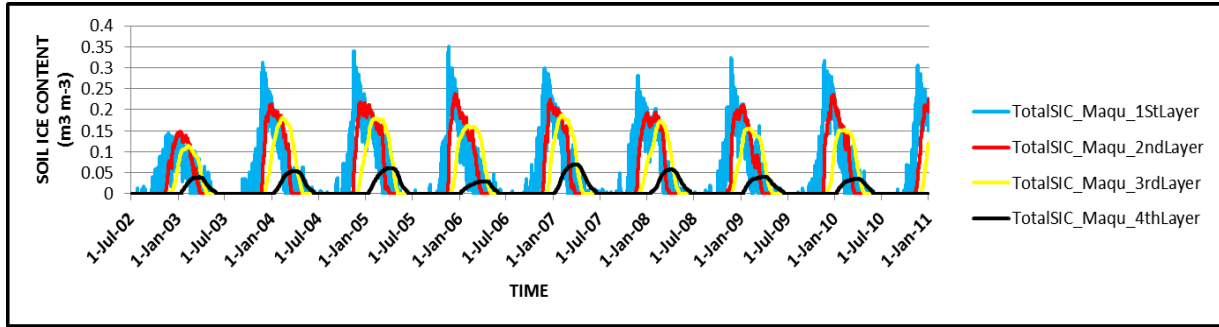


Figure 7.3.1 Simulation Results-SIC

From Figure 7.3.1 and Table 7.3.3, as soon as the temperature falls to sub-zero, gaps between TSWC and LSWC develop, for the formation of ice reduce the LSWC and make it SIC. The SIC emerges and climbs up at the mid-November of the first layer, and peak at early January. It disappears at the middle of March which last for average 120 days. When introducing the daily average, the number would decline to 95 days. The 30 minutes interval gives better profile of the daily variation. Thereafter the SIC results are more reliable on 30 minutes simulation than that of daily average.

With respect to duration of SIC at long term variation, ice firstly appears at around 275<sup>th</sup> day of a year, which is at the beginning of September, but it fluctuates and easily disappear until the beginning of October, the 300<sup>th</sup> day, to remain stable, at the first layer, depth at 5 cm. The duration is approximately 145 days. It starts around 275<sup>th</sup> day of the current year and ends up at around 75<sup>th</sup> day of the next year and would not finish thawing till 110<sup>th</sup> day of the next year.

The longest duration of ice always occurs on 4<sup>th</sup> layer, 150 days, nearly half of a year and it tends to be slightly shorter at shallower layer, and the second longest duration is at 3<sup>rd</sup> layer which is a little shorter than 149 days. However, the first layer has the shortest duration, which is 120 days and perfectly match both at start date and end date compared to the second layer. There is significantly delayed both at start and at finished line of the deeper layers. It seems the deeper the layer is, the thawing processes start at later date and shifts less often, which suggest that the deeper soil are more stable in terms of variation of SIC formation and thawing.

In Table 7.3.4, the total days of frozen cycle over the simulation period was counted, under the constraint of  $ST < 0$ . It shows that the duration of the 1<sup>st</sup> layer drops to 84.75 days at 1<sup>st</sup> layer and 107 days at second layer where there has no lag between them. The duration of third layer drops to approximately 96 days which has a lag for averagely 47 days later at the beginning of freezing and averagely 45 days at the starts of thawing. The last period of year 2010 for freezing is removed manually because it is not a complete freezing cycle. Therefore, it generates 8 complete cycles to explore the behaviour of SIC in long term variation. The duration of fourth layers astonishingly drop from 150 days of duration to 33.75 days. Since the constraint is needed, this diving number duration at 4<sup>th</sup> layers results from shortage of SIC at 4 years, 2004, 2006, 2009 2010. The problem roots into the overestimation on the soil temperature at winter where  $ST$  at the fourth layer was not collected from observation station. This may leave to be a validation on further study.

The following part is going to discuss about the duration of SIC, peak value lag time between different layers, and also the variation trend of total amount of ice since it is an important climate indicator. The presence of SIC is sensitive to the soil temperature. Considerable variation of soil ice content and liquid content results from a tiny fluctuation of soil temperature, for instance, when rises at 0.5 degree around zero, the frozen water may almost disappear when unfrozen part dramatically bounce up between soil particles. Likewise, the

more affective layers, for instance the first layer, have higher chance to generate the greatest amount of ice content both at one single day and in the whole year.



Table 7.3.3 Continuous duration of SIC of different layers (without constraint of ST&lt;0)

YEAR	TotalSIC_Maqu_1stLayer			TotalSIC_Maqu_2ndLayer			TotalSIC_Maqu_3rdLayer			TotalSIC_Maqu_4thLayer		
	Starting Date	Ending Date	Duration (Day)	Starting Date	Ending Date	Duration (Day)	Starting Date	Ending Date	Duration (Day)	Starting Date	Ending Date	Duration (Day)
2002-2003	12-Nov-02	17-Feb-03	98	16-Nov-02	26-Mar-03	131	28-Nov-02	21-Apr-03	145	14-Jan-03	26-May-03	133
2003-2004	9-Nov-03	24-Feb-04	108	22-Nov-03	16-Mar-04	116	6-Dec-03	28-Apr-04	145	12-Jan-04	11-Jun-04	152
2004-2005	29-Oct-04	7-Mar-05	130	13-Nov-04	1-Apr-05	140	30-Nov-04	4-May-05	156	11-Jan-05	13-Jun-05	154
2005-2006	4-Nov-05	24-Feb-06	113	17-Nov-05	27-Mar-06	131	29-Nov-05	1-May-06	154	6-Jan-06	30-May-06	145
2006-2007	29-Oct-06	25-Feb-07	120	20-Nov-06	26-Mar-07	127	5-Dec-06	25-Apr-07	142	8-Jan-07	16-Jun-07	160
2007-2008	30-Oct-07	6-Mar-08	129	19-Nov-07	26-Mar-08	129	4-Dec-07	3-May-08	152	16-Jan-08	18-Jun-08	155
2008-2009	29-Oct-08	12-Feb-09	107	8-Nov-08	24-Mar-09	137	29-Nov-08	1-May-09	154	9-Jan-09	15-Jun-09	158
2009-2010	11-Nov-09	8-Feb-10	90	18-Nov-09	16-Mar-10	119	2-Dec-09	24-Apr-10	144	8-Jan-10	29-May-10	142
<b>AVERAGE</b>			<b>111.88</b>			<b>128.75</b>			<b>149.00</b>			<b>149.88</b>

Table 7.3.4 Continuous duration of SIC of different layers (constraint with ST&lt;0)

YEAR	TotalSIC_Maqu_1stLayer			TotalSIC_Maqu_2ndLayer			TotalSIC_Maqu_3rdLayer			TotalSIC_Maqu_4thLayer		
	Starting Date	Ending Date	Duration (Day)	Starting Date	Ending Date	Duration (Day)	Starting Date	Ending Date	Duration (Day)	Starting Date	Ending Date	Duration (Day)
2002-2003	6-Dec-02	15-Feb-03	72	24-Nov-02	2-Mar-03	99	5-Jan-03	29-Mar-03	84	9-Mar-03	14-Apr-03	39
2003-2004	23-Nov-03	11-Feb-04	81	28-Nov-03	11-Mar-04	105	6-Jan-04	8-Apr-04	94			
2004-2005	13-Nov-04	3-Mar-05	111	19-Nov-04	15-Mar-05	117	1-Jan-05	19-Apr-05	109	9-Apr-05	10-May-05	34
2005-2006	17-Nov-05	27-Jan-06	72	21-Nov-05	15-Mar-06	115	30-Dec-05	16-Apr-06	108			
2006-2007	21-Nov-06	21-Feb-07	93	30-Nov-06	9-Mar-07	100	2-Jan-07	3-Apr-07	92	19-Mar-07	22-Apr-07	37
2007-2008	22-Nov-07	1-Mar-08	101	28-Nov-07	14-Mar-08	108	9-Jan-08	10-Apr-08	93	1-Apr-08	23-Apr-08	25
2008-2009	22-Nov-08	27-Jan-09	67	25-Nov-08	14-Mar-09	110	2-Jan-09	6-Apr-09	95			
2009-2010	17-Nov-09	5-Feb-10	81	23-Nov-09	4-Mar-10	102	1-Jan-10	4-Apr-10	94			
<b>AVERAGE</b>			<b>84.75</b>			<b>107.00</b>			<b>96.13</b>			<b>33.75</b>



### 7.3.3. Lag time and Freeze-Thaw process

**Table 7.3.5 SIC Peak date of 8 freezing cycles**

YEAR	1stLayer	2ndLayer	3rdLayer	4thLayer
2002-2003	19-Nov-02	29-Dec-02	7-Feb-03	6-Mar-03
2003-2004	26-Nov-03	23-Dec-03	5-Feb-04	20-Mar-04
2004-2005	15-Nov-04	6-Dec-04	7-Feb-05	5-Apr-05
2005-2006	18-Nov-05	11-Dec-05	30-Jan-06	2-Apr-06
2006-2007	11-Dec-06	15-Dec-06	6-Feb-07	10-Mar-07
2007-2008	26-Nov-07	31-Dec-07	14-Feb-08	17-Apr-08
2008-2009	24-Nov-08	3-Jan-09	18-Jan-09	27-Mar-09
2009-2010	20-Nov-09	20-Dec-09	19-Jan-10	12-Apr-10
<b>AVERAGE</b>	<b>23-Nov</b>	<b>21-Dec</b>	<b>1-Feb</b>	<b>27-Mar</b>

Different to the soil temperature, the lag time of SIC peak date is immense (Table 7.3.3 and Table 7.3.4), nearly one month from the first and second layer. The value of ST is around 2 days the lag time in the duration gaps between different layers are likewise, as shown in the table7.3.5.

**Table 7.3.6 Lag time of SIC peak date between different layers (Days per year)**

YEAR	Lag1_2	Lag2_3	Lag3_4
2002-2003	40	40	27
2003-2004	27	44	44
2004-2005	21	63	57
2005-2006	23	50	62
2006-2007	4	53	32
2007-2008	35	45	63
2008-2009	40	15	68
2009-2010	30	30	83
<b>AVERAGE</b>	<b>27.5</b>	<b>42.5</b>	<b>54.5</b>

From table 7.3.6 and 7.3.7, a discrepancy between SIC duration and SIC peaking date occurs. The lag time of duration and peak date is different, which suggests the shapes of the waves are different. With respect to the shape of SIC, it is likely to have sharp and thin peak at the first layer and short but wide wave at the bottom layer. This difference reveals that it has strong and quick response in terms of freeze-thaw process which has shorter duration at the top dynamic layer, but has relative delayed and long lasting process at deeper layers which produce less amount of ice.

**Table 7.3.7 Lag time in start and end dates of freezing between different layers**

lag time(Days)	between 1st and 2nd		between 2nd and 3rd		
	year	start date	end date	start date	end date
2002	1	0	51	41	
2003	0	8	44	45	
2004	0	0	48	45	
2005	1	0	42	54	
2006	0	0	42	39	
2007	0	0	49	40	
2008	0	0	41	56	
2009	2	0	43	57	
<b>Average</b>	<b>0.5</b>	<b>1</b>	<b>45</b>	<b>47.125</b>	

#### 7.4. Active Layer Thickness

When temperature is below freezing point, a frost front forms between the frozen and unfrozen soil, and the frozen part usually at top soil is named of Active Layer. Active Layer Thickness (ALT) is an important indicator for monitoring climate change, which represents the boundary of the sensitive layers where freezing and thawing transition takes place. Therefore ALT varies from summer to winter since this depth representing existence of SIC depends on the variation temperature.

After constraint of soil temperature, over year 2002 to 2010, the changes in ALT at the first three layer is not much variable since the shape of eight cycles are very much identical. Similar to that of the analysis of previous section, the first layer starts to be frozen at late October or early November, but the frost front takes a long time penetrating into the 4<sup>th</sup> layer. What is shown on the figure 7.4.1 indicates the incomplete cycles for 4<sup>th</sup> layer. The overestimation of soil temperature at 4<sup>th</sup> layer gives rise to only 4 out of 8 freezing/thawing cycles observed, which are the year of 2003, 2005, 2008, and 2009. The longest duration appears at layer 3 and shortest at layer 1.

In conclusion, there are no significant changes from ALT to forecast a warmer or colder situation on SRYR from this study. In other words, the global warming is not shown on the figure of ALT, for one possible reason is that the simulation period is not long enough for climate study. Another major factor for such no-changes in ALT pattern over years is the layering deployed by Noah LSM. It indicates that with the current configuration of layering the Noah LSM cannot provide detailed enough information to reflect the subtle changes in ALT(e.g. mm scale) The bar chart below represents the variation of ALT over the 8.5 freezing-thawing cycles.

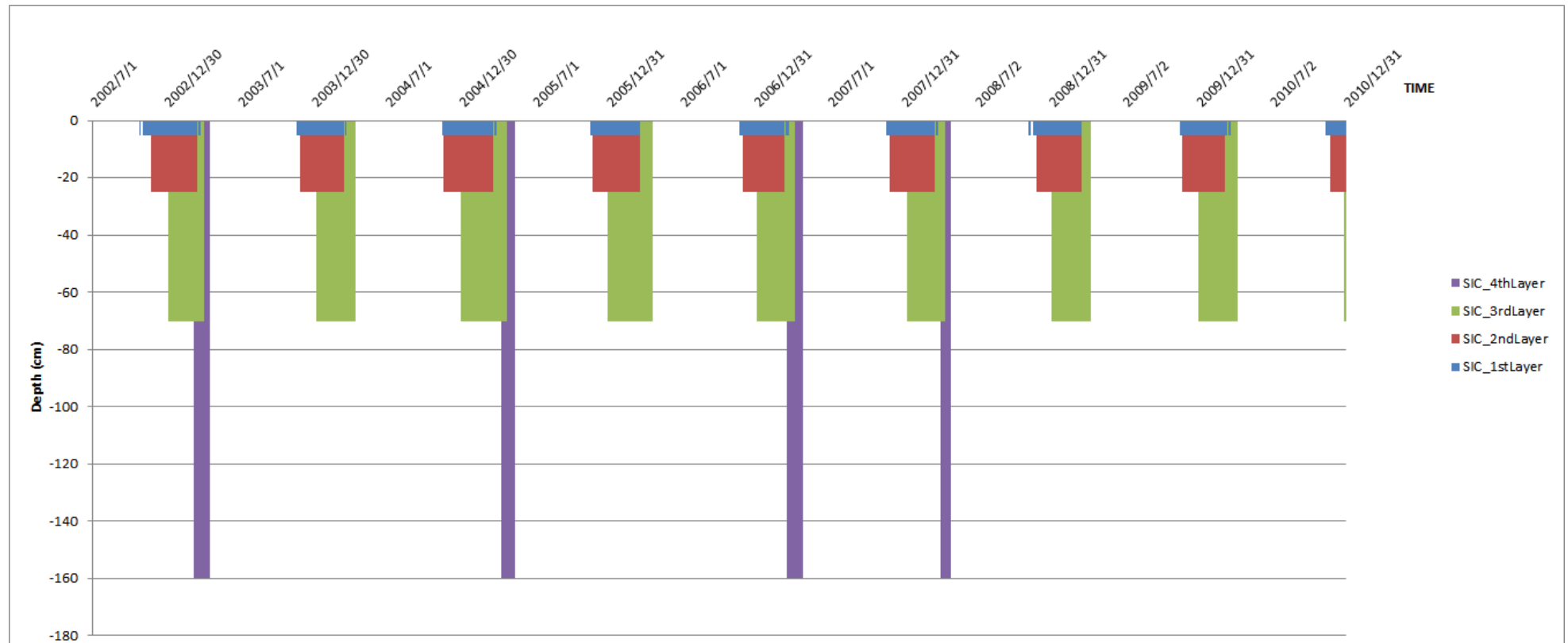


Figure 7.4.1 Active layer thickness at long term variation



## 8. CONCLUSION

### 8.1. Review on the thesis

This thesis targets on analysing the freeze-thaw process over the SRYR on Tibetan Plateau, from 2002 to 2011. The in-situ measurement of LSWC can help to validate the NOAH LSM simulation results, constructing a long-term simulation of freeze-thaw process.

The validation result seems to prove the fact that the LSM applied is reliable at the study area both on soil moisture and soil temperature simulations. Nevertheless, in order to capture a more precise description on the freeze-thaw cycle, the Noah LSM need further updated parameterization on hydrothermal dynamics. It was found that the NOAH LSM generates SIC even with the ST above freezing point. This may be caused by the current not well tuned parameterization of freezing/thawing process in the model and deserves further investigations.

For Noah simulation results concerned in this research, the four variables, LSWC, TSWC, SIC, ST, also with the ALT are representing a stable stage over long term variation. And freeze-thaw processes over a seasonal frozen area have vertical difference over different layer. The top layer tends to show more dynamic freeze-thaw processes, which is strong and in high frequency of variation on the amount, but a short duration of frozen period. The bottom layer provides a longer freezing duration but lower amount of ice is formed.

### 8.2. Conclusions and subsequent work

**Table 8.2.1 Duration of SIC in comparably constraint**

Duration of SIC(Days per Year)	Before Constraint		After Constraint	
	Source data	daily average	Source data	daily average
1st Layer	111.88	168.63	84.75	93.13
2nd Layer	128.75	129.38	107.00	107.50
3rd Layer	149.00	150.13	96.13	97.25
4th Layer	149.88	150.88	33.75	31.75

The main problems of the Noah LSM simulation results are from the prediction of SIC (both the amount of ice content and the duration). When under the constraint of  $ST < 0$  degree, the freezing duration was cut off short at 3<sup>rd</sup> and 4<sup>th</sup> layer, from 149 days per run to 96, and 150 days to 33.75 days, respectively. This problem roots into the overestimation on the soil temperature at winter. Since the insufficient days of low temperature under  $0\text{ }^{\circ}\text{C}$ , the duration of SIC would not be precisely predicted until a corresponding well simulated ST at deep layers.

Besides the temperature constraint problem, underestimation on the amount of SIC as the depth increased lack of observation data at rather deep soil. Since digging over frozen soil is a harsh task, the solution is to produce more precise estimation on available data on soil moisture and soil temperature by the usability of bias-correction method. Therefore, subsequent research is mainly about the bias-correction and validation on freezing/thawing parameterization to improve the performance of Noah LSM on the simulation of SM/ST.

---

**LIST OF REFERENCES**


---

- Arenson, L. U., Johansen, M. M., & Springman, S. M. (2004). Effects of volumetric ice content and strain rate on shear strength under triaxial conditions for frozen soil samples. *Permafrost and Periglacial Processes*, 15(3), 261–271. <http://doi.org/10.1002/ppp.498>
- Arenson, L. U., Springman, S. M., & Sego, D. C. (2007). The Rheology of Frozen Soils. *Applied Rheology*. Retrieved from [https://www.researchgate.net/profile/Lukas\\_Arenson/publication/228623901\\_The\\_rheology\\_of\\_frozen\\_soils/links/54ecb1840cf27bfd7714d4f.pdf](https://www.researchgate.net/profile/Lukas_Arenson/publication/228623901_The_rheology_of_frozen_soils/links/54ecb1840cf27bfd7714d4f.pdf)
- Baker, B., & Lawson, R. P. (2006). Improvement in Determination of Ice Water Content from Two-Dimensional Particle Imagery. Part I: Image-to-Mass Relationships. *Journal of Applied Meteorology and Climatology*, 45(9), 1282–1290. <http://doi.org/10.1175/JAM2398.1>
- Boike, J., & Roth, K. (1997). Time domain reflectometry as a field method for measuring water content and soil water electrical conductivity at a continuous permafrost site. *Permafrost and Periglacial Processes*, 8(4), 359–370. [http://doi.org/10.1002/\(SICI\)1099-1530\(199710/12\)8:4<359::AID-PPP261>3.0.CO;2-S](http://doi.org/10.1002/(SICI)1099-1530(199710/12)8:4<359::AID-PPP261>3.0.CO;2-S)
- Cheng, Q., Sun, Y., Qin, Y., Xue, X., Cai, X., Sheng, W., & Zhao, Y. (2013). In situ measuring soil ice content with a combined use of dielectric tube sensor and neutron moisture meter in a common access tube. *Agricultural and Forest Meteorology*, 171-172, 249–255. <http://doi.org/10.1016/j.agrformet.2012.12.004>
- Ek, M. B. (2003). Implementation of Noah land surface model advances in the National Centers for Environmental Prediction operational mesoscale Eta model. *Journal of Geophysical Research*, 108(D22), 8851. <http://doi.org/10.1029/2002JD003296>
- Flerchinger, G. N., Seyfried, M. S., & Hardegee, S. P. (2006). Using Soil Freezing Characteristics to Model Multi-Season Soil Water Dynamics. *Vadose Zone Journal*, 5(4), 1143. <http://doi.org/10.2136/vzj2006.0025>
- Harlan, R. L. (1973). Analysis of coupled heat-fluid transport in partially frozen soil. *Water Resources Research*, 9(5), 1314–1323. <http://doi.org/10.1029/WR009i005p01314>
- Hayhoe, H. N., Topp, G. C., & Bailey, W. G. (1983). Measurement of soil water contents and frozen soil depth during a thaw using time-domain reflectometry. *Atmosphere-Ocean*, 21(3), 299–311. <http://doi.org/10.1080/07055900.1983.9649170>
- He, H., & Dyck, M. (2013). Application of Multiphase Dielectric Mixing Models for Understanding the Effective Dielectric Permittivity of Frozen Soils. *Vadose Zone Journal*, 12(1). <http://doi.org/10.2136/vzj2012.0060>
- Jame, Y.-W., & Norum, D. I. (1980). Heat and mass transfer in a freezing unsaturated porous medium. *Water Resources Research*, 16(4), 811–819. <http://doi.org/10.1029/WR016i004p00811>
- Koren, V., Schaake, J., Mitchell, K., Duan, Q.-Y., Chen, F., & Baker, J. M. (1999). A parameterization of snowpack and frozen ground intended for NCEP weather and climate models. *Journal of Geophysical Research: Atmospheres*, 104(D16), 19569–19585. <http://doi.org/10.1029/1999JD900232>

- Kurylyk, B. L., & Watanabe, K. (2013). The mathematical representation of freezing and thawing processes in variably-saturated, non-deformable soils. *Advances in Water Resources*, *60*, 160–177. <http://doi.org/10.1016/j.advwatres.2013.07.016>
- Lundin, L.-C. (1990). Hydraulic properties in an operational model of frozen soil. *Journal of Hydrology*, *118*(1-4), 289–310. [http://doi.org/10.1016/0022-1694\(90\)90264-X](http://doi.org/10.1016/0022-1694(90)90264-X)
- Mahrt, L., & Pan, H. (1984). A two-layer model of soil hydrology. *Boundary-Layer Meteorology*, *29*(1), 1–20. <http://doi.org/10.1007/BF00119116>
- Pan, H.-L., & Mahrt, L. (1987). Interaction between soil hydrology and boundary-layer development. *Boundary-Layer Meteorology*, *38*(1-2), 185–202. <http://doi.org/10.1007/BF00121563>
- Poutou, E., Krinner, G., Genthon, C., & de Noblet-Ducoudré, N. (2004). Role of soil freezing in future boreal climate change. *Climate Dynamics*, *23*(6), 621–639. <http://doi.org/10.1007/s00382-004-0459-0>
- Schaake, J. C., Koren, V. I., Duan, Q.-Y., Mitchell, K., & Chen, F. (1996). Simple water balance model for estimating runoff at different spatial and temporal scales. *Journal of Geophysical Research: Atmospheres*, *101*(D3), 7461–7475. <http://doi.org/10.1029/95JD02892>
- Spaans, E. J. A., & Baker, J. M. (1995). Examining the use of time domain reflectometry for measuring liquid water content in frozen soil. *Water Resources Research*, *31*(12), 2917–2925. <http://doi.org/10.1029/95WR02769>
- Stähli, M., & Stadler, D. (1997). Measurement of water and solute dynamics in freezing soil columns with time domain reflectometry. *Journal of Hydrology*, *195*(1-4), 352–369. [http://doi.org/10.1016/S0022-1694\(96\)03227-1](http://doi.org/10.1016/S0022-1694(96)03227-1)
- Su, Z., Wen, J., Dente, L., van der Velde, R., Wang, L., Ma, Y., ... Hu, Z. (2011). The Tibetan Plateau observatory of plateau scale soil moisture and soil temperature (Tibet-Obs) for quantifying uncertainties in coarse resolution satellite and model products. *Hydrology and Earth System Sciences*, *15*(7), 2303–2316. <http://doi.org/10.5194/hess-15-2303-2011>
- Watanabe, K., & Wake, T. (2009). Measurement of unfrozen water content and relative permittivity of frozen unsaturated soil using NMR and TDR. *Cold Regions Science and Technology*, *59*(1), 34–41. <http://doi.org/10.1016/j.coldregions.2009.05.011>
- Yoshikawa, K., & Overduin, P. P. (2005). Comparing unfrozen water content measurements of frozen soil using recently developed commercial sensors. *Cold Regions Science and Technology*, *42*(3), 250–256. <http://doi.org/10.1016/j.coldregions.2005.03.001>
- Zheng, D. (2015). *Water and Heat Exchanges on the Tibetan Plateau Observation and Modeling of the Yellow River Source Region*.
- Zheng, D., van der Velde, R., Su, Z., Wang, X., Wen, J., Booij, M. J., ... Chen, Y. (2015). Augmentations to the Noah Model Physics for Application to the Yellow River Source Area. Part II: Turbulent Heat Fluxes and Soil Heat Transport. *Journal of Hydrometeorology*, *16*(6), 2677–2694. <http://doi.org/10.1175/JHM-D-14-0199.1>
- Zheng, D., Van der Velde, R., Su, Z., Wen, J., Booij, M. J., Hoekstra, A. Y., & Wang, X. (2015). Under-canopy turbulence and root water uptake of a Tibetan meadow ecosystem modeled by Noah-MP. *Water Resources Research*, *51*(7), 5735–5755. <http://doi.org/10.1002/2015WR017115>

Zreda, M., Desilets, D., Ferré, T. P. a, & Scott, R. L. (2008). Measuring soil moisture content non-invasively at intermediate spatial scale using cosmic-ray neutrons. *Geophysical Research Letters*, 35(21). <http://doi.org/10.1029/2008GL035655>

## APPENDIX

## FIGURES

## Validation Results

Reds for Simulated Soil moisture and soil temperature results and Blues are observation results of three layers at depth 5 cm, 25 cm and 70 cm from July 1, 2008 till Jun 30, 2009 as pixel-wise simulation.

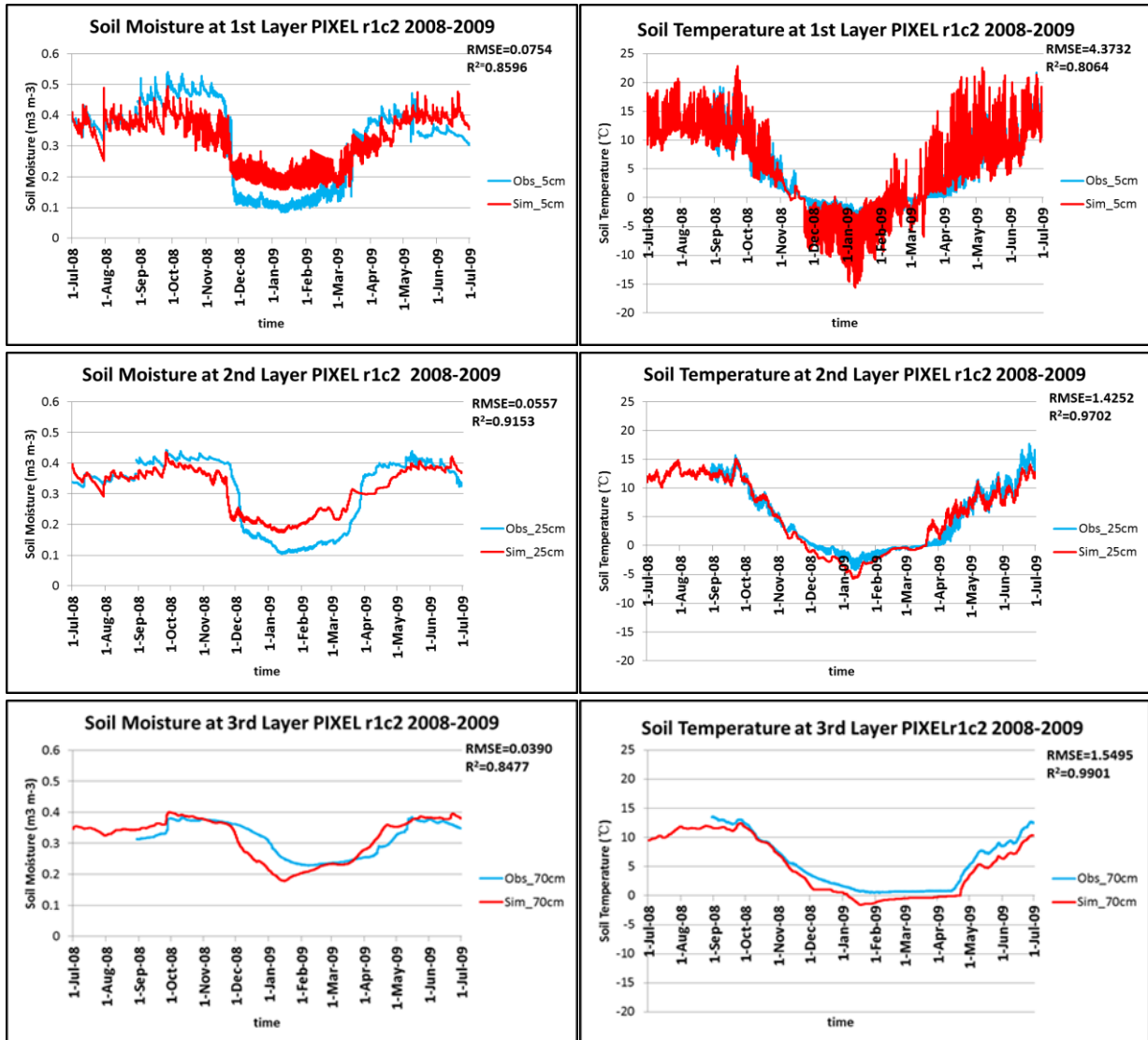


Figure 1.1 Validation results on Station CST05 (ROW 1 COLUMN 2)

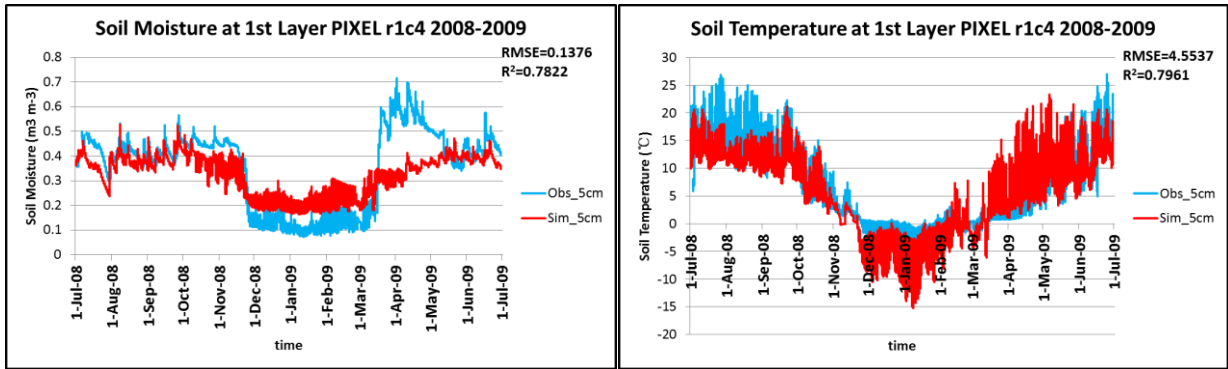


Figure 2.2 Validation results on Station NST04-NST05 (ROW 1 COLUMN 4)

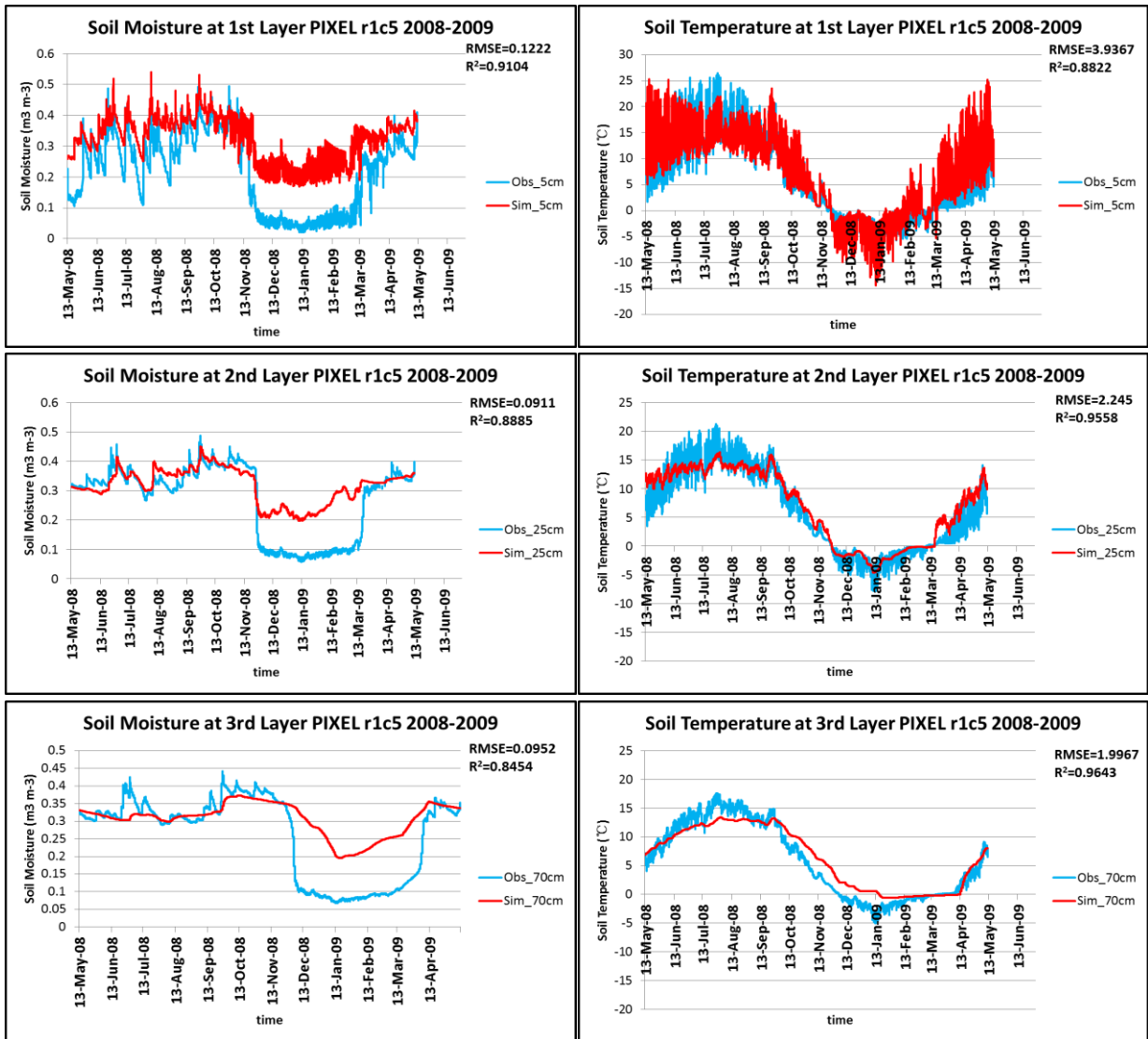


Figure 3.3 Validation results on Station CST02 (ROW 1 COLUMN 5)

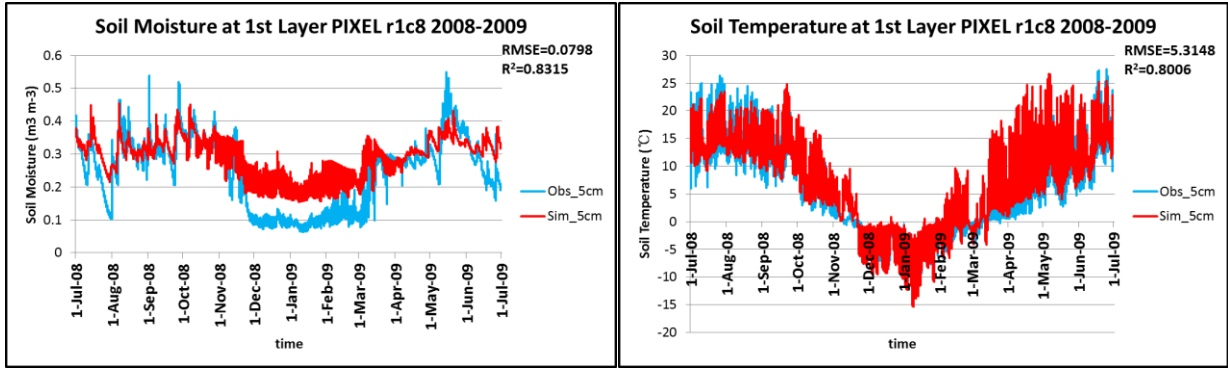


Figure 4.4 Validation results on Station NST11-NST12 (ROW 1 COLUMN 8)

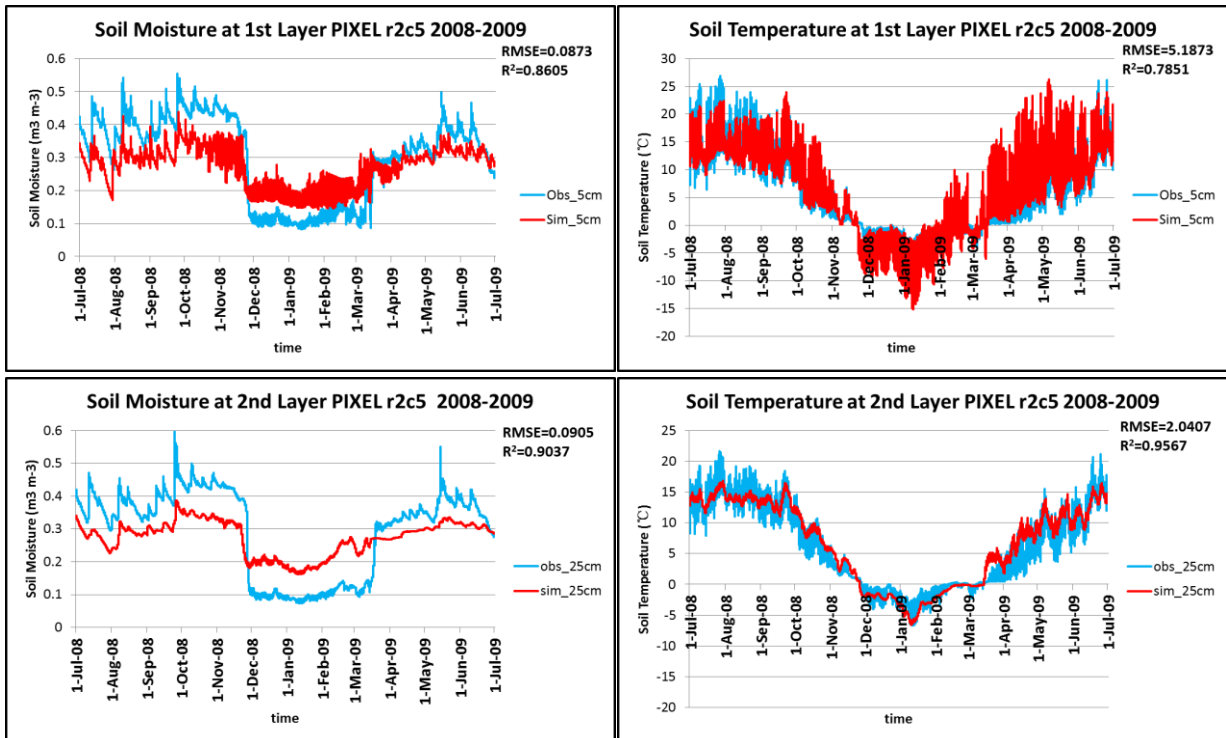


Figure 5.5 Validation results on Station NST03 (ROW 2 COLUMN 5)

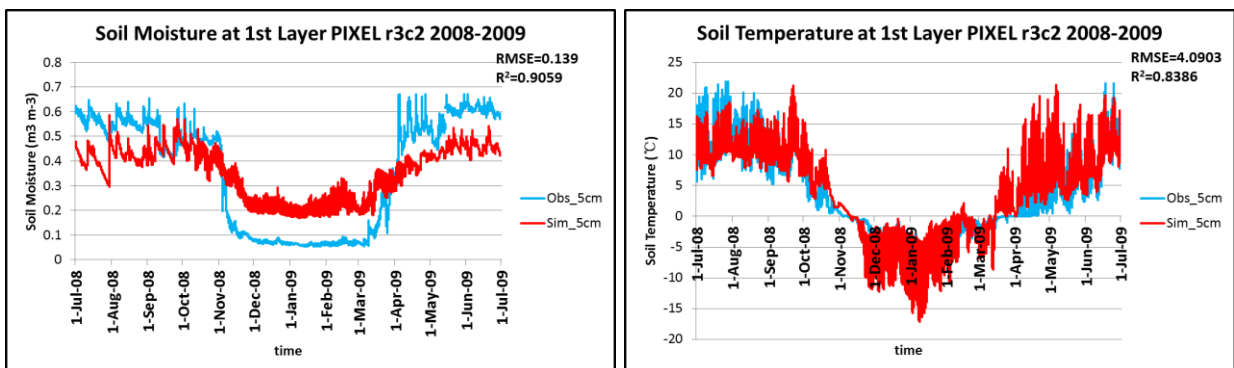


Figure 6.6 Validation results on Station NST15 (ROW 3 COLUMN 2)

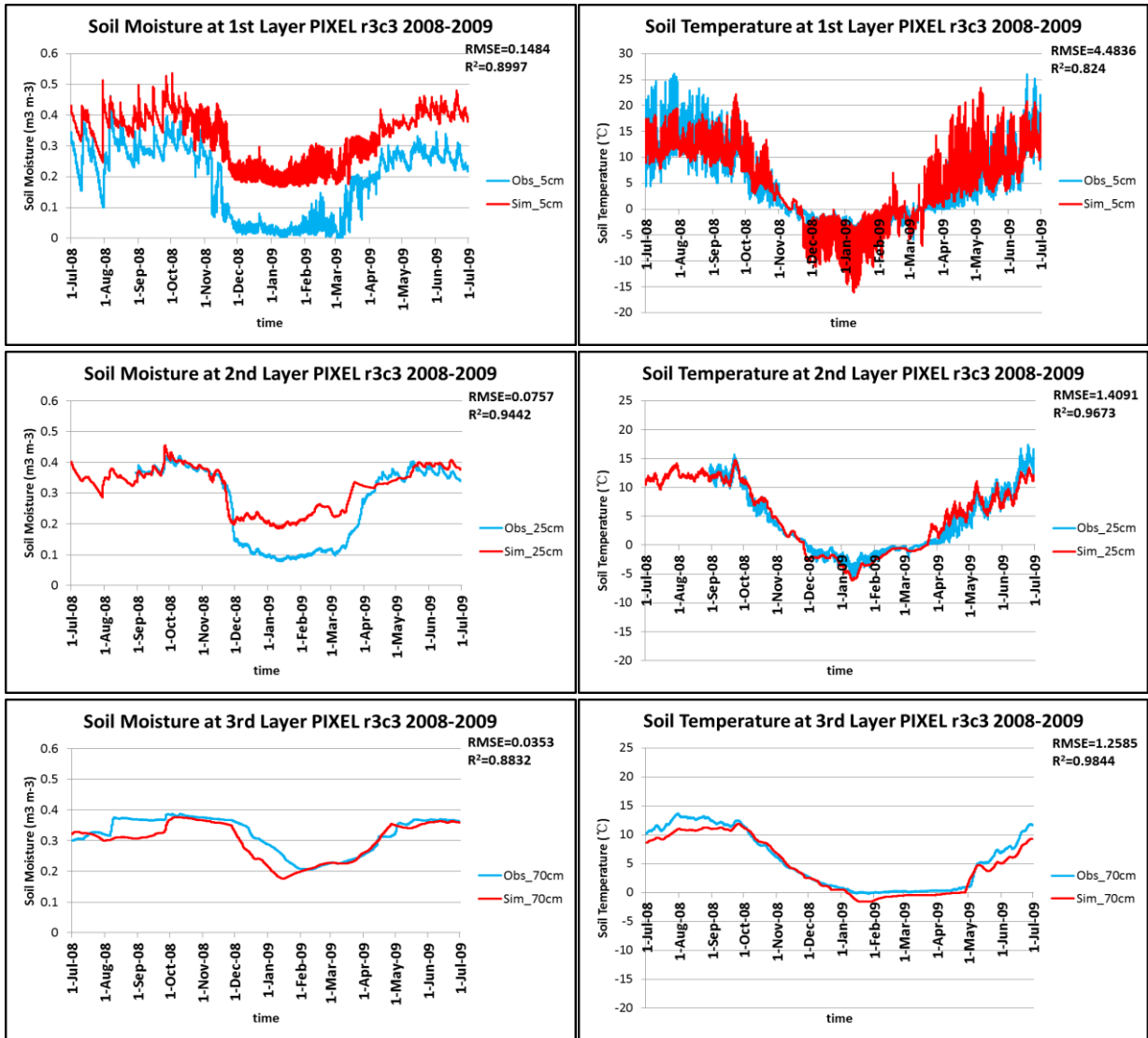


Figure 7.7 Validation results on Station CST03 (ROW 3 COLUMN 3)

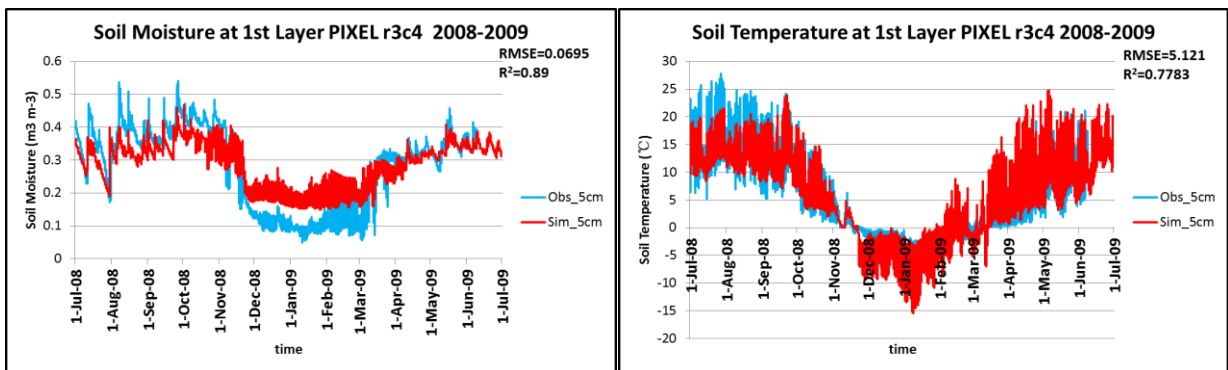


Figure 8.8 Validation results on Station NST14 (ROW 3 COLUMN 4)

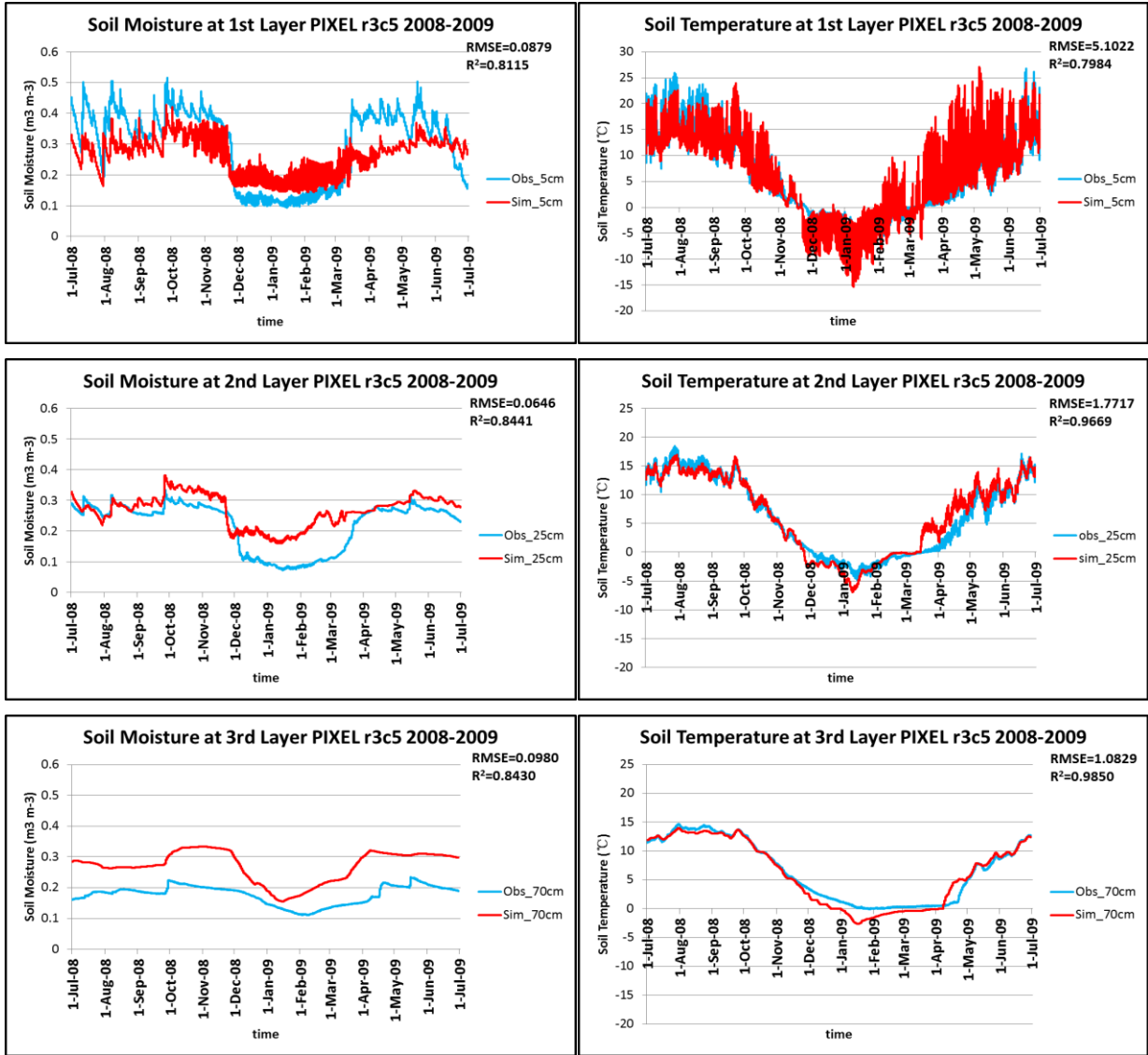


Figure 9.9 Validation results on Station CST01 (ROW 3 COLUMN 5)

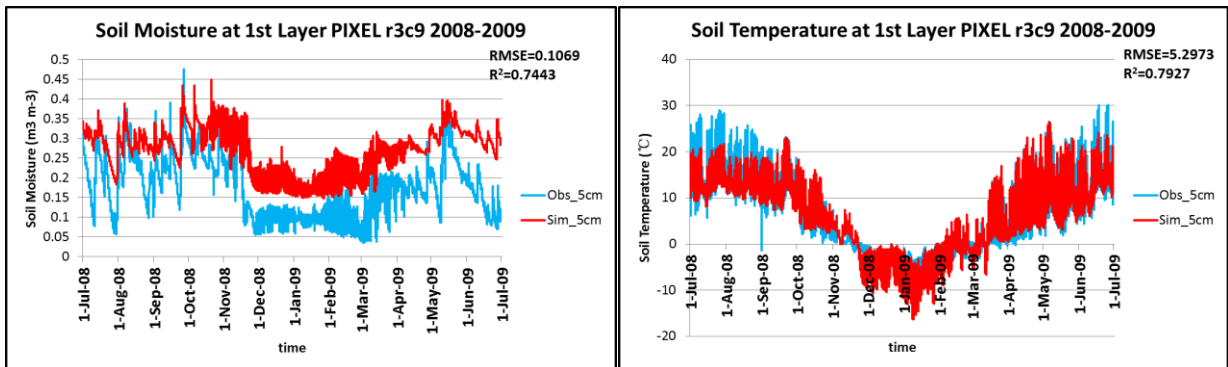


Figure 10.10 Validation results on Station NST09- NST 10 (ROW 3 COLUMN 9)

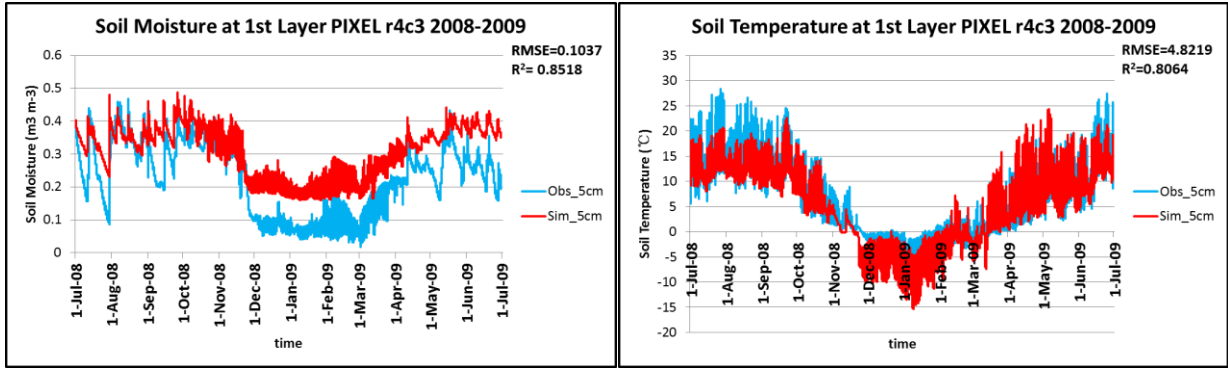


Figure 11.11 Validation results on Station NST13 (ROW 4 COLUMN 3)

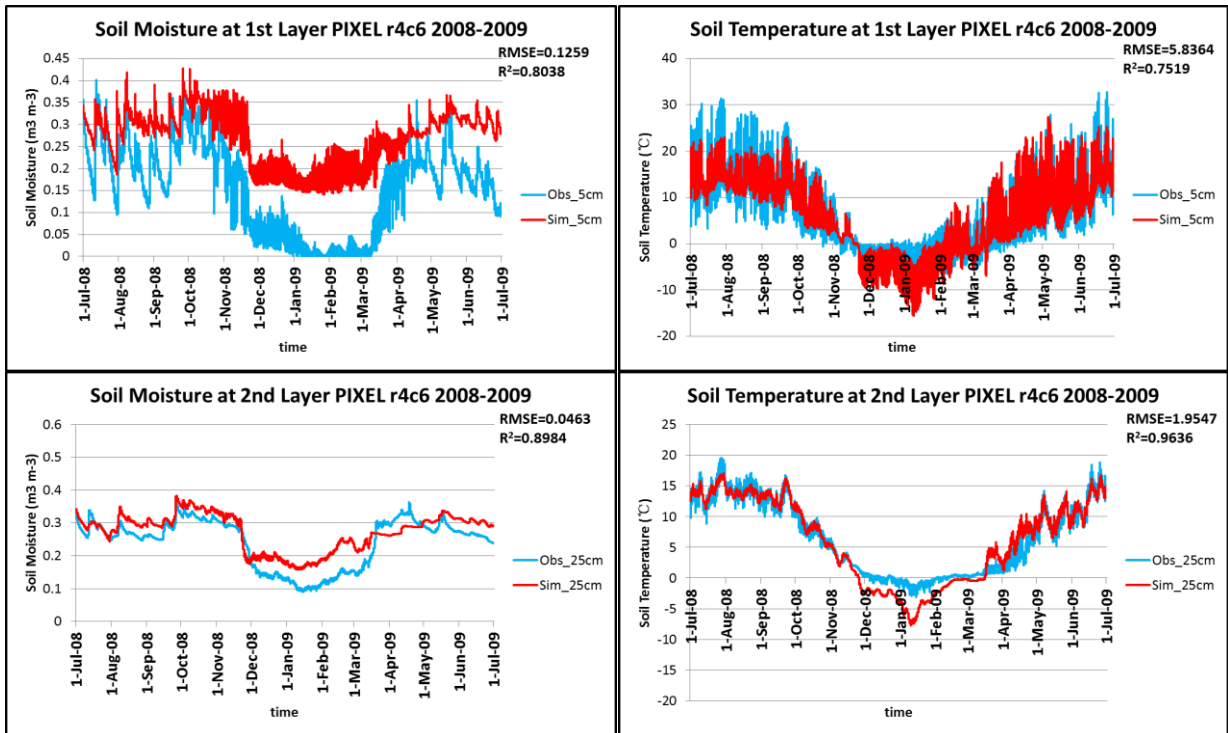


Figure 12.12 Validation results on Station NST06 (ROW 4 COLUMN 6)

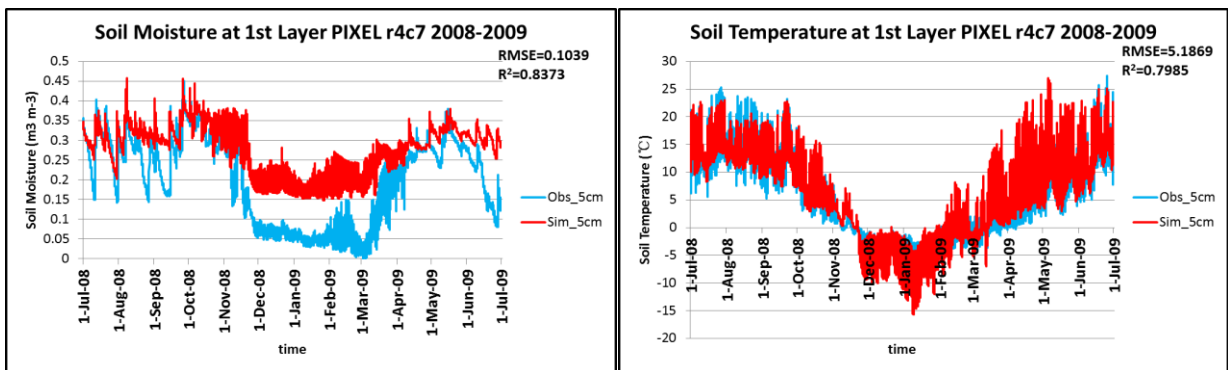


Figure 13.13 Validation results on Station NST07 (ROW 4 COLUMN 7)

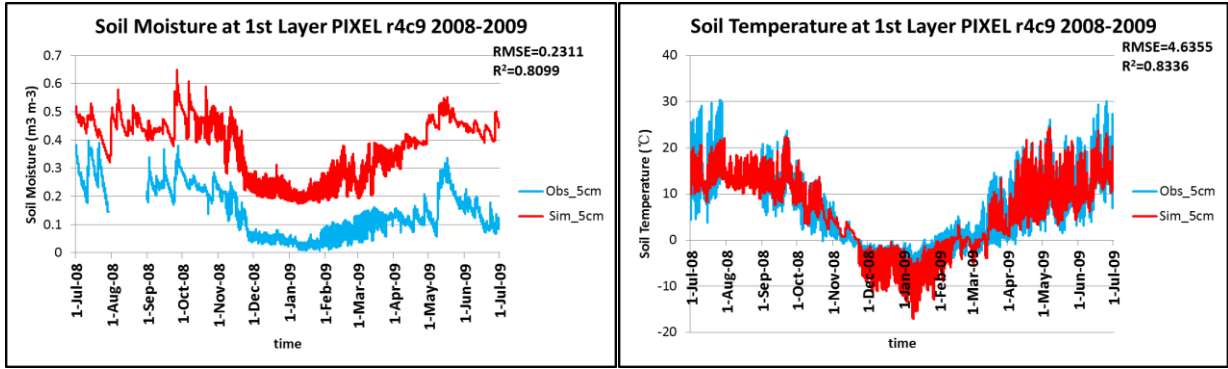


Figure 14.14 Validation results on Station NST08 (ROW 4 COLUMN 9)

Simulation Results

Long-term simulation results present at 4 different variables, LSWC, TSWC, SIC and ST as SRYR domain lumped value

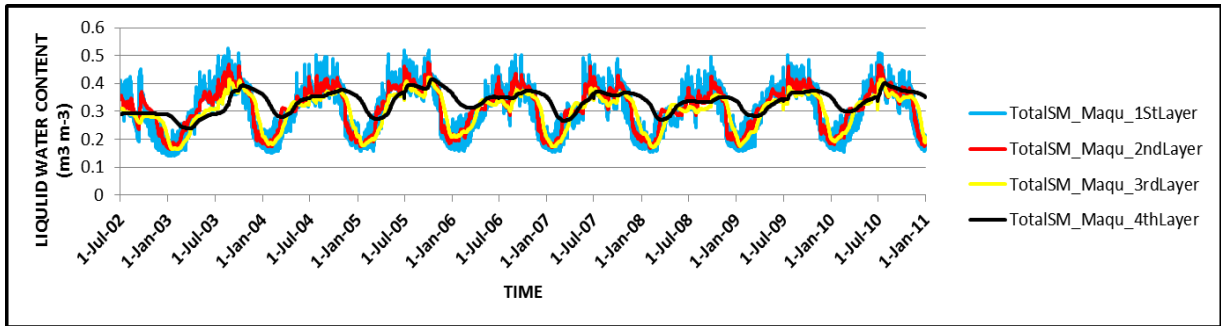


Figure 2.15 Simulation Results-LSWC

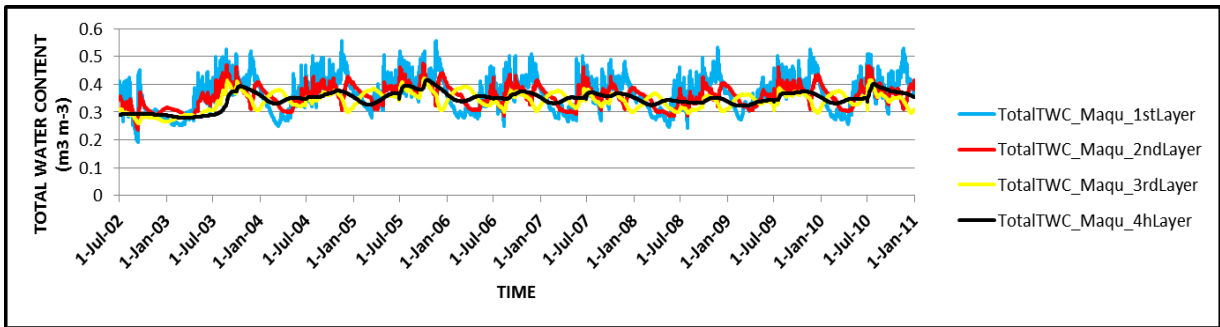


Figure 16.2 Simulation Results-TSWC

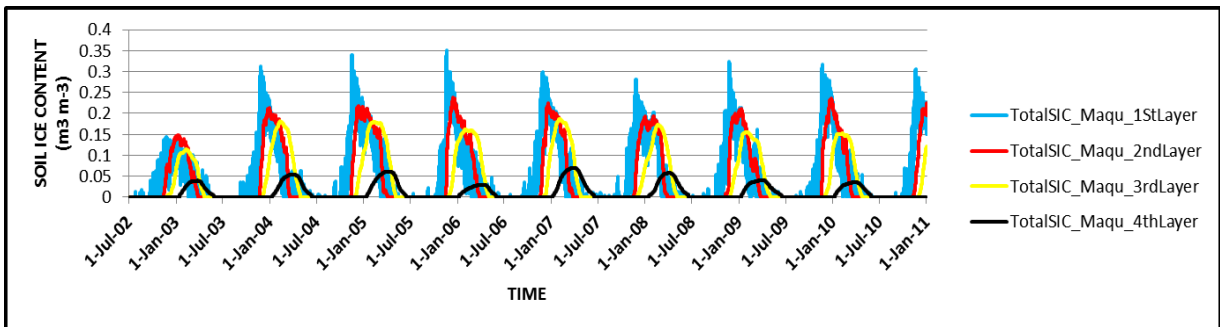


Figure 17.3 Simulation Results-SIC

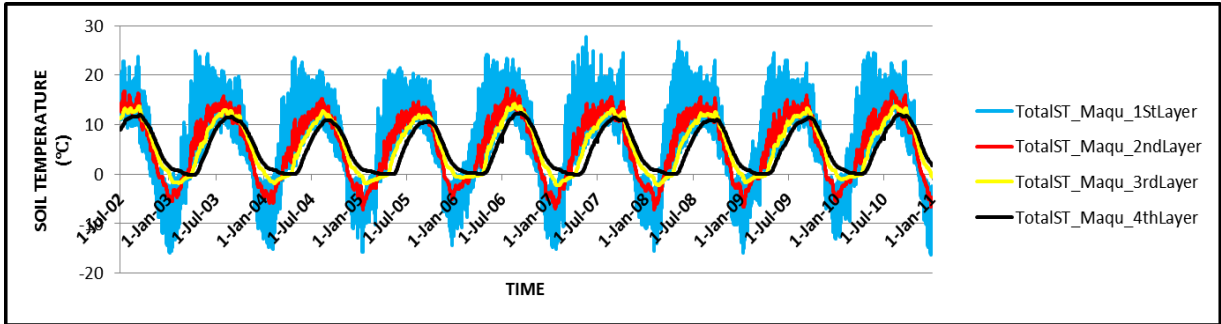


Figure 18.4 Simulation Results-ST

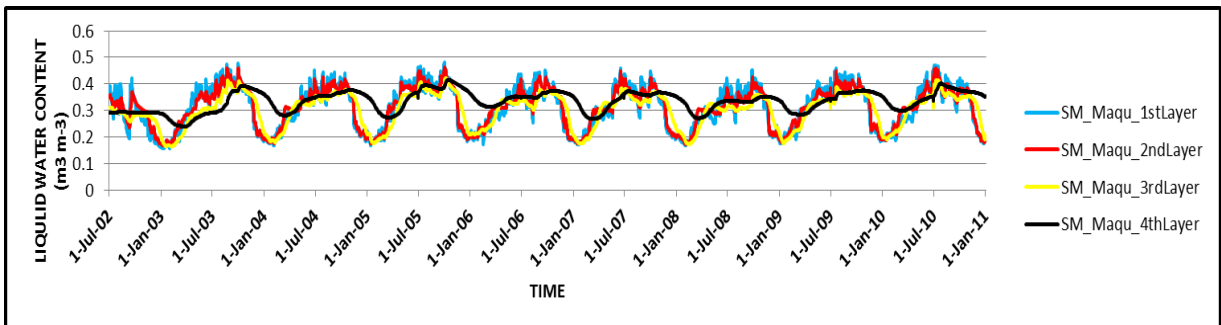


Figure 19.5 Simulation Results at Daily Average-LSWC

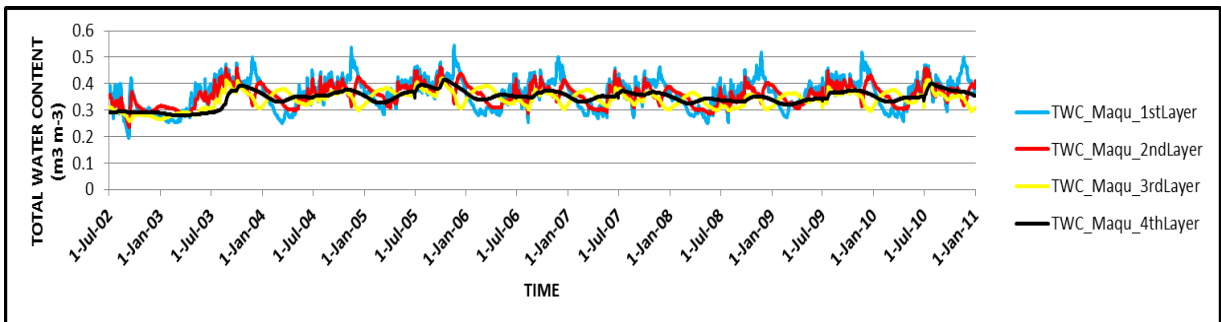


Figure 20.6 Simulation Results at Daily Average-TSWC

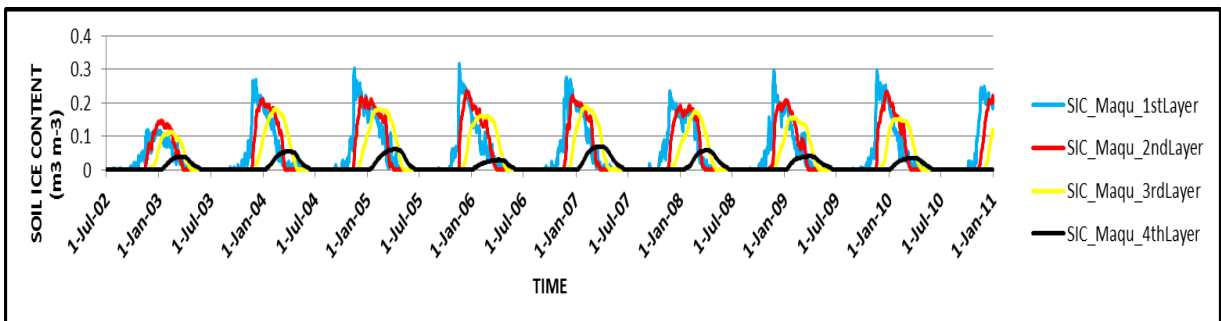


Figure 21.7 Simulation Results at Daily Average-SIC

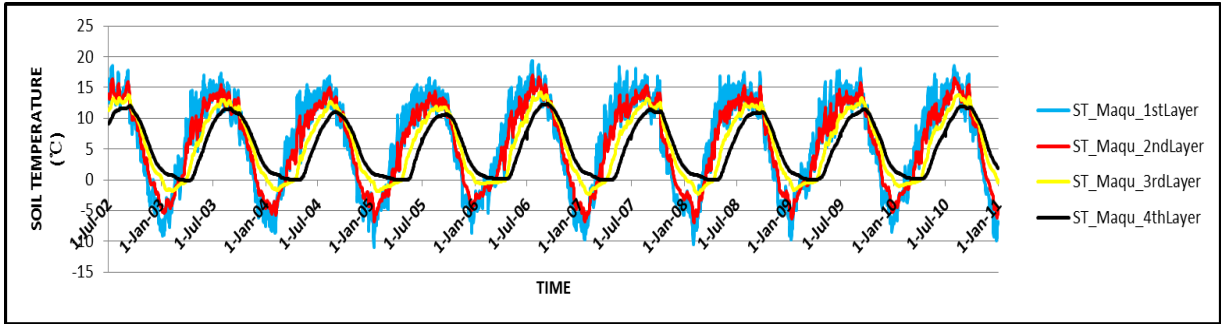


Figure 22.8 Simulation Results at Daily Average-ST

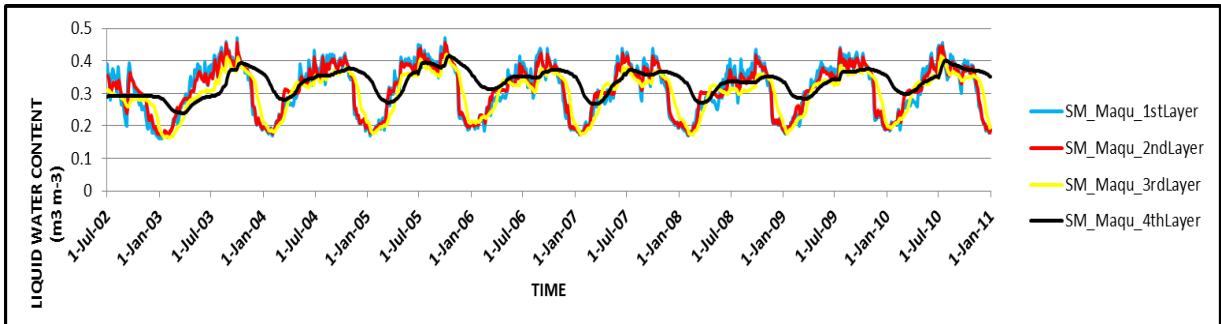


Figure 23.9 3-Day Average-LSWC

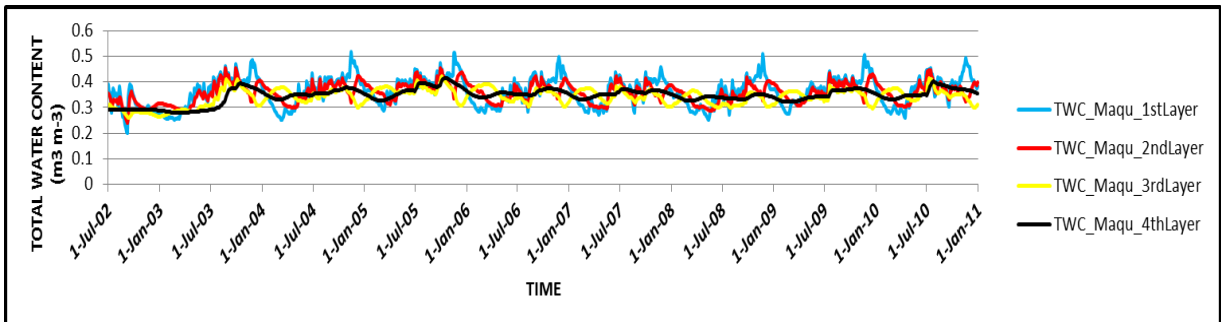


Figure 24.10 3-Day Average-TSWC

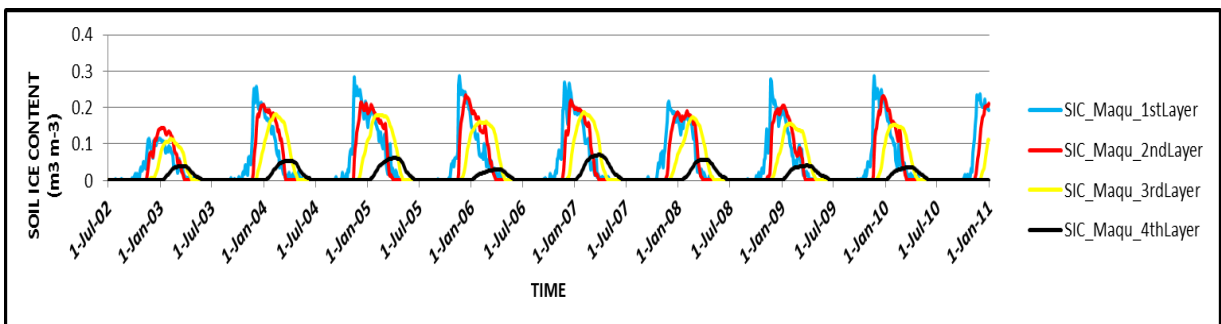


Figure 25.11 3-Day Average-SIC

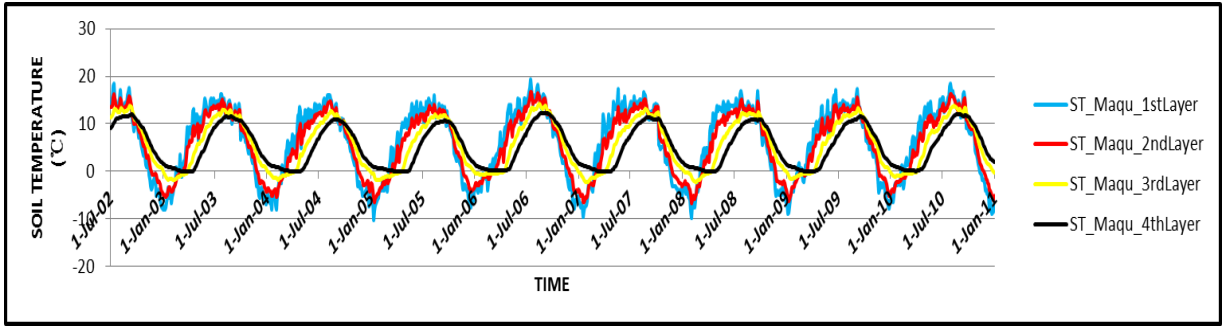


Figure 26.12 3-Day Average-ST

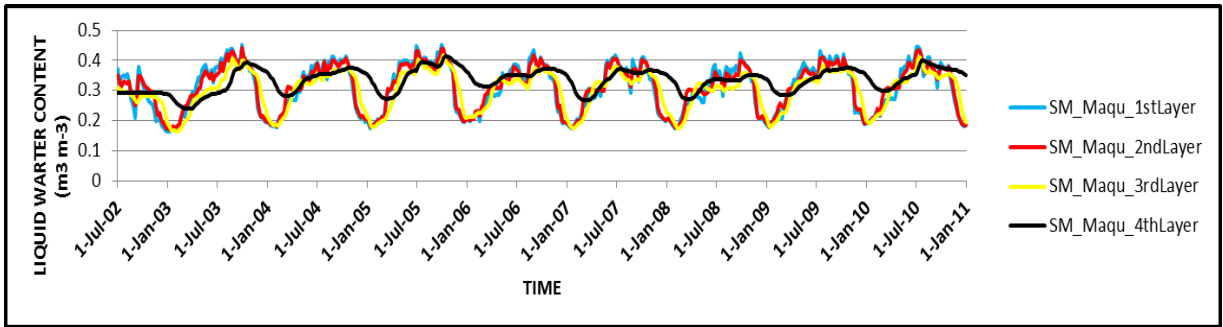


Figure 27.13 Weekly Average-LSWC

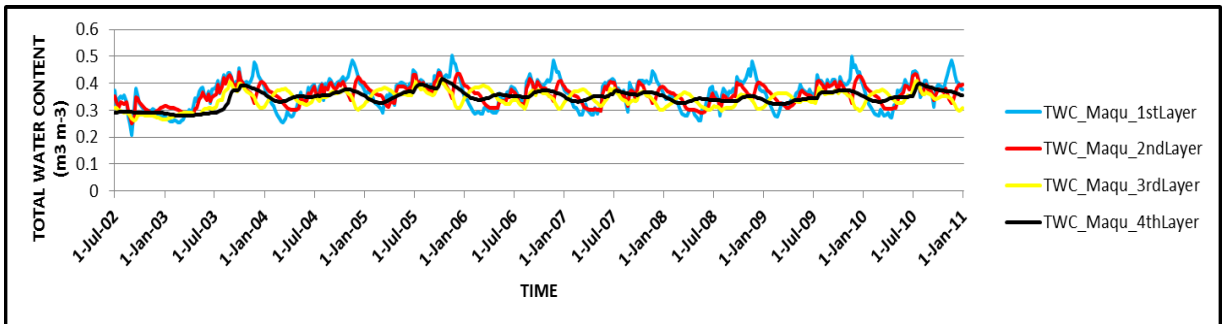


Figure 28.14 Weekly Average-TSWC

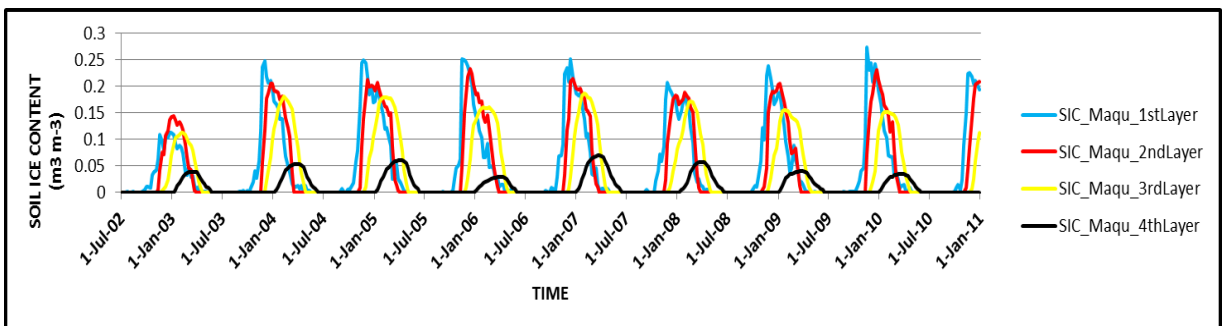


Figure 29.15 Weekly Average-SIC

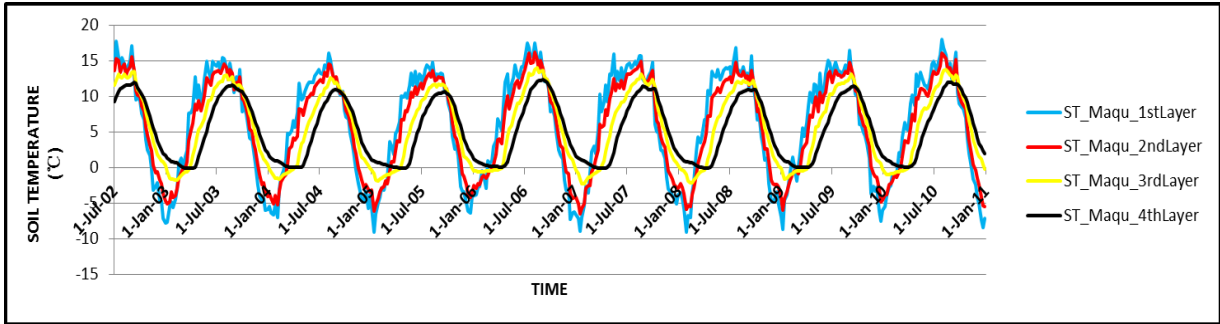


Figure 30.16 Weekly Average-ST

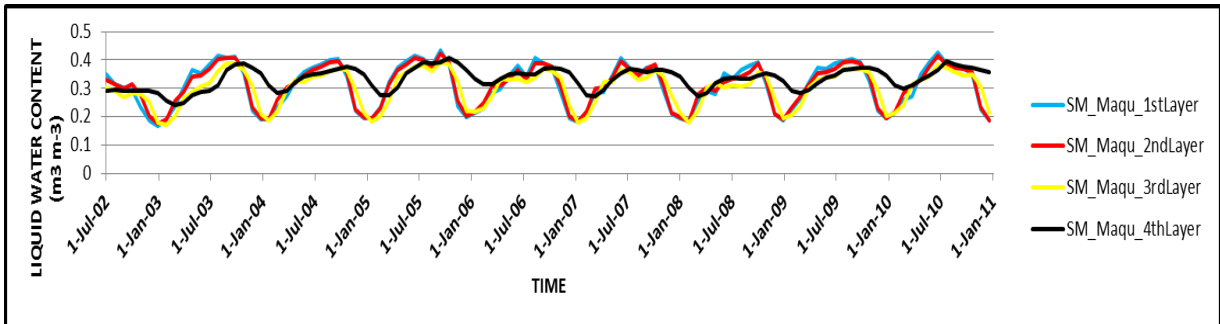


Figure 31.17 Monthly Average-LSWC

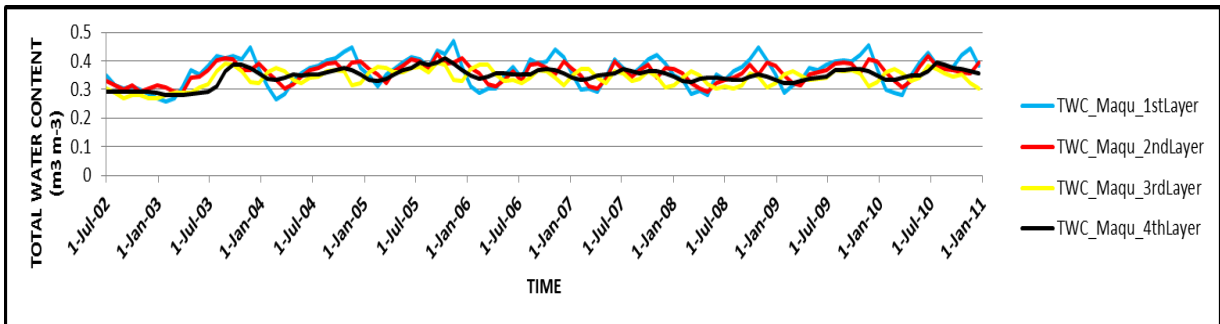


Figure 32.18 Monthly Average-TSWC

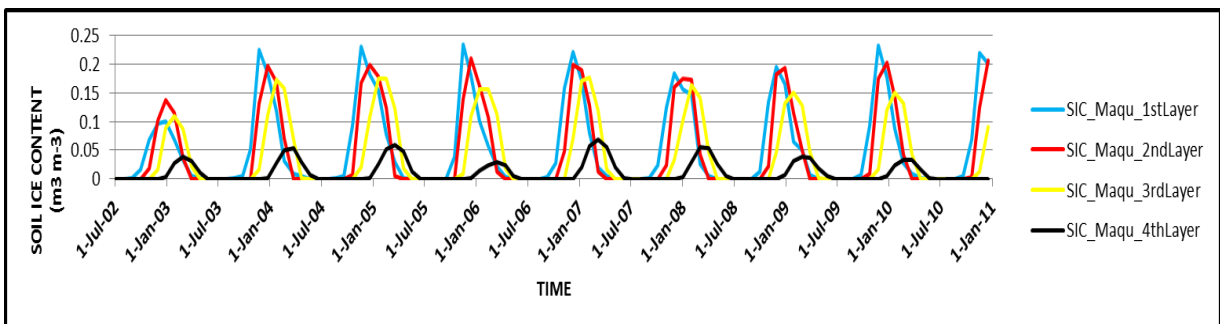


Figure 33.19 Monthly Average-SIC

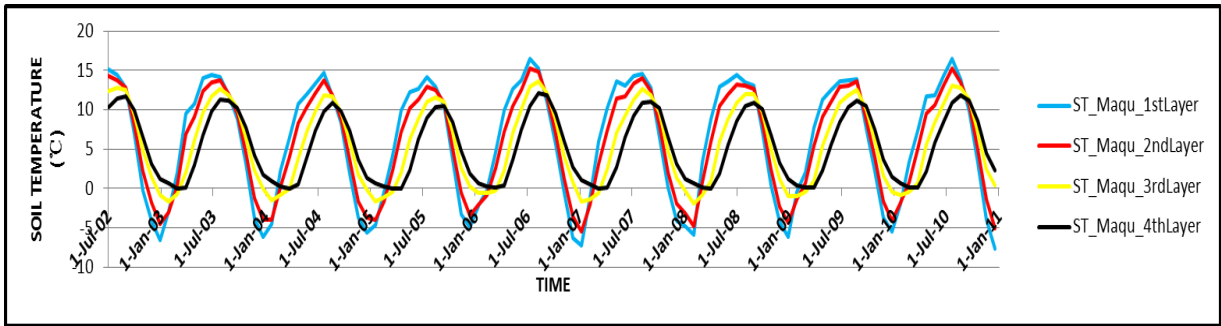


Figure 34.20 Monthly Average-ST

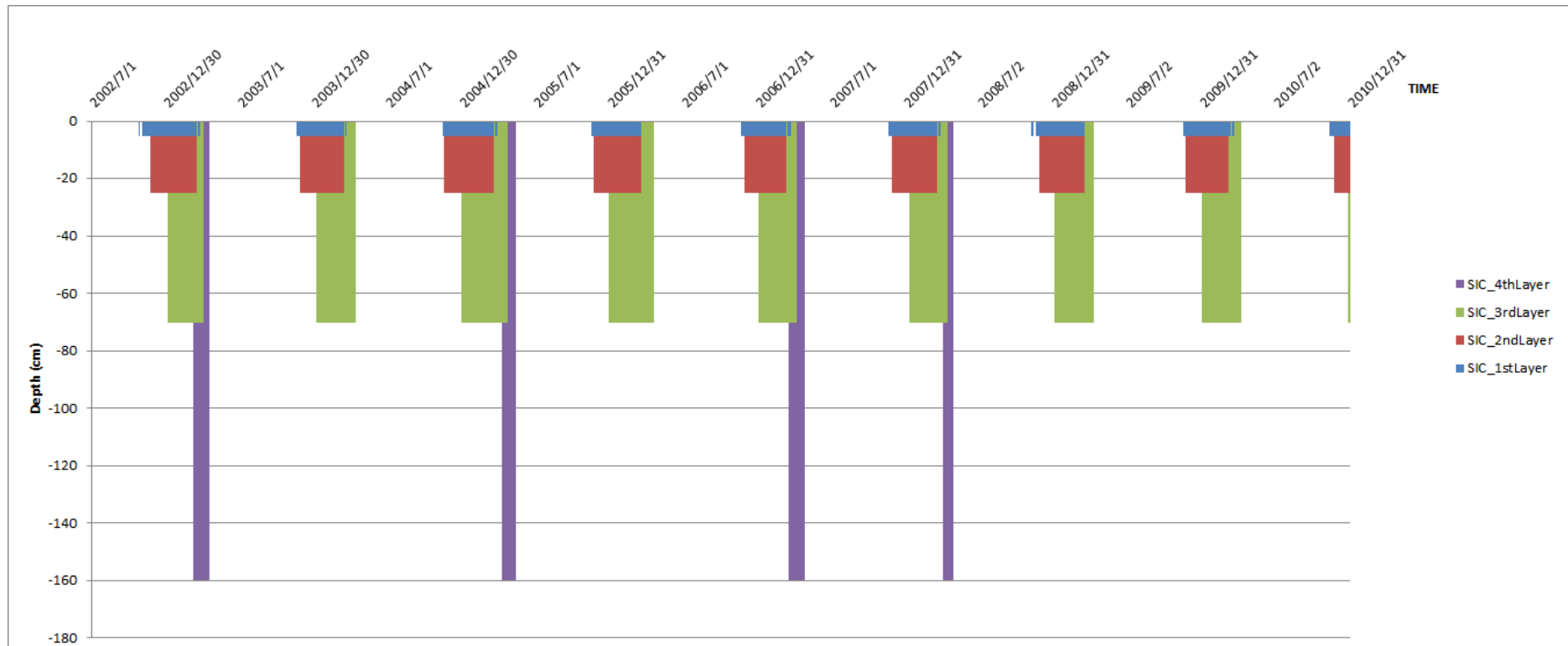


Figure 35.1 Active layer thickness at long term variation



**Table 1.1 Monitoring stations and its locating pixels**

Station	LAT	LON	LAT	LON	row	column
CST01	33°53'14.16"N	102°08'25.62"E	33.88337267	102.1334045	3	5
CST02	33°40'42.60"N	102°08'18.66"E	33.666785	102.1333852	1	5
CST03	33°52'17.82"N	101°58'15.66"E	33.86671617	101.9667102	3	3
CST04	33°46'12.84"N	101°43'52.98"E	33.76670233	101.7168138	2	1
CST05	33°40'46.50"N	101°53'21.78"E	33.66679583	101.8833938	1	2
NST01	33°53'22.68"N	102°08'27.48"E	33.88339633	102.1334097	3	5
NST02	33°53'04.74"N	102°08'32.28"E	33.88339633	102.133423	3	5
NST03	33°46'00.54"N	102°08'50.52"E	33.76666817	102.1334737	2	5
NST04	33°37'52.14"N	102°03'25.56"E	33.6168115	102.050071	1	4
NST05	33°38'05.10"N	102°03'34.68"E	33.6333475	102.0500963	1	4
NST06	34°00'29.70"N	102°16'53.58"E	34.0000825	102.2668155	4	6
NST07	33°59'13.74"N	102°21'37.20"E	33.9833715	102.3501033	4	7
NST08	33°58'19.44"N	102°36'31.08"E	33.96672067	102.6000863	4	9
NST09	33°54'38.64"N	102°33'00.78"E	33.90010733	102.5500022	3	9
NST10	33°51'07.74"N	102°34'25.44"E	33.8500215	102.5667373	3	9
NST11	33°41'33.18"N	102°28'36.12"E	33.6834255	102.466767	1	8
NST12	33°37'16.02"N	102°28'00.36"E	33.61671117	102.4666677	1	8
NST13	34°01'53.70"N	101°56'31.44"E	34.01681583	101.9334207	4	3
NST14	33°55'35.64"N	102°07'42.78"E	33.91676567	102.1167855	3	4
NST15	33°51'26.10"N	101°53'28.08"E	33.8500725	101.8834113	3	2

**Table 2.1 Valid SIC dates of the simulation result**

Numbers of Days	Total		Daily Average	
	SIC>0.004	ST<0	SIC>0.004	ST<0
1st Layer	1422.40	868.13	1622	866
2nd Layer	1084.33	906.38	1086	907
3rd Layer	1227.19	778.96	1231	780
4th Layer	1205.58	131.13	1207	131

**Table 3.2 Valid SIC percentage of the simulation result**

Percentage of cycle	Total		Daily Average	
	SIC>0.004	ST<0	SIC>0.004	ST<0
1st Layer	45.82%	27.97%	52.26%	27.90%
2nd Layer	34.93%	29.20%	34.99%	29.22%
3rd Layer	39.54%	25.10%	39.66%	25.13%
4th Layer	38.84%	4.22%	38.89%	4.22%

**Table 4.3 Bottom ST dates of the simulation result**

YEAR	1stLayer	2ndLayer	3rdLayer	4thLayer
2002-2003	19-Nov-02	29-Dec-02	7-Feb-03	6-Mar-03
2003-2004	26-Nov-03	23-Dec-03	5-Feb-04	20-Mar-04
2004-2005	15-Nov-04	6-Dec-04	7-Feb-05	5-Apr-05
2005-2006	18-Nov-05	11-Dec-05	30-Jan-06	2-Apr-06
2006-2007	11-Dec-06	15-Dec-06	6-Feb-07	10-Mar-07
2007-2008	26-Nov-07	31-Dec-07	14-Feb-08	17-Apr-08
2008-2009	24-Nov-08	3-Jan-09	18-Jan-09	27-Mar-09
2009-2010	20-Nov-09	20-Dec-09	19-Jan-10	12-Apr-10
<b>AVERAGE</b>	<b>23-Nov</b>	<b>21-Dec</b>	<b>1-Feb</b>	<b>27-Mar</b>

**Table 5.4 Bottom ST and lag time of the simulation result (Days)**

YEAR	Lag1_2	Lag2_3	Lag3_4
2002-2003	40	40	27
2003-2004	27	44	44
2004-2005	21	63	57
2005-2006	23	50	62
2006-2007	4	53	32
2007-2008	35	45	63
2008-2009	40	15	68
2009-2010	30	30	83
<b>AVERAGE</b>	<b>27.5</b>	<b>42.5</b>	<b>54.5</b>

**Table 6.5 SIC lag time between different layers**

lag time(Days)	between 1st and 2nd		between 2nd and 3rd	
	start date	end date	start date	end date
2002	1	0	51	41
2003	0	8	44	45
2004	0	0	48	45
2005	1	0	42	54
2006	0	0	42	39
2007	0	0	49	40
2008	0	0	41	56
2009	2	0	43	57
<b>Average</b>	<b>0.5</b>	<b>1</b>	<b>45</b>	<b>47.125</b>

Table 7.6 Continuous duration of SIC of different layers (source data, with constraint)

YEAR	TotalSIC_Maqu_1stLayer			TotalSIC_Maqu_2ndLayer			TotalSIC_Maqu_3rdLayer			TotalSIC_Maqu_4thLayer		
	Starting Date	Ending Date	Duration (Day)	Starting Date	Ending Date	Duration (Day)	Starting Date	Ending Date	Duration (Day)	Starting Date	Ending Date	Duration (Day)
2002-2003	12-Nov-02	17-Feb-03	98	16-Nov-02	26-Mar-03	131	28-Nov-02	21-Apr-03	145	14-Jan-03	26-May-03	133
2003-2004	9-Nov-03	24-Feb-04	108	22-Nov-03	16-Mar-04	116	6-Dec-03	28-Apr-04	145	12-Jan-04	11-Jun-04	152
2004-2005	29-Oct-04	7-Mar-05	130	13-Nov-04	1-Apr-05	140	30-Nov-04	4-May-05	156	11-Jan-05	13-Jun-05	154
2005-2006	4-Nov-05	24-Feb-06	113	17-Nov-05	27-Mar-06	131	29-Nov-05	1-May-06	154	6-Jan-06	30-May-06	145
2006-2007	29-Oct-06	25-Feb-07	120	20-Nov-06	26-Mar-07	127	5-Dec-06	25-Apr-07	142	8-Jan-07	16-Jun-07	160
2007-2008	30-Oct-07	6-Mar-08	129	19-Nov-07	26-Mar-08	129	4-Dec-07	3-May-08	152	16-Jan-08	18-Jun-08	155
2008-2009	29-Oct-08	12-Feb-09	107	8-Nov-08	24-Mar-09	137	29-Nov-08	1-May-09	154	9-Jan-09	15-Jun-09	158
2009-2010	11-Nov-09	8-Feb-10	90	18-Nov-09	16-Mar-10	119	2-Dec-09	24-Apr-10	144	8-Jan-10	29-May-10	142
<b>AVERAGE</b>			<b>111.88</b>			<b>128.75</b>			<b>149.00</b>			<b>149.88</b>

Table 8.7 Continuous duration of SIC of different layers (daily average, without constraint)

YEAR	TotalSIC_Maqu_1stLayer			TotalSIC_Maqu_2ndLayer			TotalSIC_Maqu_3rdLayer			TotalSIC_Maqu_4thLayer		
	Starting Date	Ending Date	Duration (Day)	Starting Date	Ending Date	Duration (Day)	Starting Date	Ending Date	Duration (Day)	Starting Date	Ending Date	Duration (Day)
2002-2003	18-Oct-02	3-Apr-03	168	15-Nov-02	27-Mar-03	133	28-Nov-02	21-Apr-03	145	13-Jan-03	26-May-03	134
2003-2004	17-Oct-03	8-Apr-04	175	22-Nov-03	17-Mar-04	117	6-Dec-03	28-Apr-04	145	12-Jan-04	12-Jun-04	153
2004-2005	21-Oct-04	4-Apr-05	166	13-Nov-04	1-Apr-05	140	29-Nov-04	5-May-05	158	10-Jan-05	14-Jun-05	156
2005-2006	20-Oct-05	17-Apr-06	180	17-Nov-05	28-Mar-06	132	28-Nov-05	1-May-06	155	6-Jan-06	31-May-06	146
2006-2007	23-Oct-06	28-Mar-07	157	20-Nov-06	26-Mar-07	127	4-Dec-06	26-Apr-07	144	8-Jan-07	16-Jun-07	160
2007-2008	17-Oct-07	7-Apr-08	174	19-Nov-07	26-Mar-08	129	3-Dec-07	3-May-08	153	16-Jan-08	18-Jun-08	155
2008-2009	19-Oct-08	6-Apr-09	170	8-Nov-08	24-Mar-09	137	28-Nov-08	1-May-09	155	9-Jan-09	16-Jun-09	159
2009-2010	13-Oct-09	20-Mar-10	159	18-Nov-09	17-Mar-10	120	1-Dec-09	25-Apr-10	146	7-Jan-10	30-May-10	144
<b>AVERAGE</b>			<b>168.63</b>			<b>129.38</b>			<b>150.13</b>			<b>150.88</b>

Table 9.8 Continuous duration of SIC of different layers (Source data, with constraint)

YEAR	TotalSIC_Maqu_1stLayer			TotalSIC_Maqu_2ndLayer			TotalSIC_Maqu_3rdLayer			TotalSIC_Maqu_4thLayer		
	Starting Date	Ending Date	Duration (Day)	Starting Date	Ending Date	Duration (Day)	Starting Date	Ending Date	Duration (Day)	Starting Date	Ending Date	Duration (Day)
2002-2003	6-Dec-02	15-Feb-03	72	24-Nov-02	2-Mar-03	99	5-Jan-03	29-Mar-03	84	9-Mar-03	14-Apr-03	39
2003-2004	23-Nov-03	11-Feb-04	81	28-Nov-03	11-Mar-04	105	6-Jan-04	8-Apr-04	94			
2004-2005	13-Nov-04	3-Mar-05	111	19-Nov-04	15-Mar-05	117	1-Jan-05	19-Apr-05	109	9-Apr-05	10-May-05	34
2005-2006	17-Nov-05	27-Jan-06	72	21-Nov-05	15-Mar-06	115	30-Dec-05	16-Apr-06	108			
2006-2007	21-Nov-06	21-Feb-07	93	30-Nov-06	9-Mar-07	100	2-Jan-07	3-Apr-07	92	19-Mar-07	22-Apr-07	37
2007-2008	22-Nov-07	1-Mar-08	101	28-Nov-07	14-Mar-08	108	9-Jan-08	10-Apr-08	93	1-Apr-08	23-Apr-08	25
2008-2009	22-Nov-08	27-Jan-09	67	25-Nov-08	14-Mar-09	110	2-Jan-09	6-Apr-09	95			
2009-2010	17-Nov-09	5-Feb-10	81	23-Nov-09	4-Mar-10	102	1-Jan-10	4-Apr-10	94			
<b>AVERAGE</b>			<b>84.75</b>			<b>107.00</b>			<b>96.13</b>			<b>33.75</b>

Table 10.9 Continuous duration of SIC of different layers (Daily average, with constraint)

YEAR	TotalSIC_Maqu_1stLayer			TotalSIC_Maqu_2ndLayer			TotalSIC_Maqu_3rdLayer			TotalSIC_Maqu_4thLayer		
	Starting Date	Ending Date	Duration (Day)	Starting Date	Ending Date	Duration (Day)	Starting Date	Ending Date	Duration (Day)	Starting Date	Ending Date	Duration (Day)
2002-2003	14-Nov-02	17-Feb-03	96	23-Nov-02	2-Mar-03	100	5-Jan-03	30-Mar-03	85	9-Mar-03	15-Apr-03	37
2003-2004	22-Nov-03	23-Feb-04	94	28-Nov-03	11-Mar-04	105	5-Jan-04	8-Apr-04	95			
2004-2005	13-Nov-04	5-Mar-05	113	18-Nov-04	15-Mar-05	118	31-Dec-04	19-Apr-05	110	8-Apr-05	11-May-05	33
2005-2006	16-Nov-05	1-Feb-06	78	21-Nov-05	15-Mar-06	115	29-Dec-05	16-Apr-06	109			
2006-2007	20-Nov-06	24-Feb-07	97	29-Nov-06	9-Mar-07	101	1-Jan-07	4-Apr-07	94	18-Mar-07	22-Apr-07	35
2007-2008	21-Nov-07	2-Mar-08	103	28-Nov-07	14-Mar-08	108	9-Jan-08	11-Apr-08	94	1-Apr-08	23-Apr-08	22
2008-2009	21-Nov-08	9-Feb-09	81	25-Nov-08	14-Mar-09	110	1-Jan-09	6-Apr-09	96			
2009-2010	16-Nov-09	6-Feb-10	83	22-Nov-09	4-Mar-10	103	31-Dec-09	4-Apr-10	95			
<b>AVERAGE</b>			<b>93.13</b>			<b>107.5</b>			<b>97.25</b>			<b>31.75</b>